U. S. Atomic Energy Commission
Docket 50-3
Exhibit K-5A2

# BAW-133

# FUEL ELEMENT STRUCTURAL DESIGN AND MANUFACTURE FOR THE CONSOLIDATED EDISON THORIUM REACTOR PLANT

September 1960





THE BABCOCK & WILCOX COMPANY

ATOMIC ENERGY DIVISION

## DISCLAIMER

U. S. Atomic Energy Commission
Docket 50-3
Exhibit K-5A2

BAW-133

# FUEL ELEMENT STRUCTURAL DESIGN AND MANUFACTURE FOR THE CONSOLIDATED EDISON THORIUM REACTOR PLANT

September 1960

By
D. M. Collings
D. K. Gestson
C. Andrea
H. D. Ferris
R. L. Boyer
G. C. Larson

Approved by: H. R. Rock
H. R. Rock, Chief
Mechanisms
Engineering

Approved by: W C Gumprich
W. C. Gumprich, Manager
Engineering Department

PREPARED FOR
THE CONSOLIDATED EDISON COMPANY OF NEW YORK
BY
THE BABCOCK & WILCOX COMPANY
ATOMIC ENERGY DIVISION
Lynchburg, Virginia

537-002

## CROSS REFERENCE INDEX

This Cross Reference Index has been prepared to key the supplementary material to the information which is contained in the Hazards Summary Report dated January, 1960, Exhibit K-5 (Rev-1) filed with Amendment No. 10 to Consolidated Edison's Application for Licenses.

## SECTION 2 - REACTOR DESIGN

| 2.1 - REACTOR DESCRIPTION | EXHIBIT NO. |
|---|---|
| 2.1.1 Reactor Vessel and Its Internal Structure | |
| Consolidated Edison Thorium Reactor Reactor Vessel Internal Components Design (Report BAW-136) | K-5A1 |
| 2.1.2 Fuel Element Design | |
| Fuel Element Structural Design and Manufacture for the Consolidated Edison Thorium Reactor Plant (Report BAW-133) | K-5A2 |
| 2.1.3 Control Rods, Fixed Shim Rods and Flux Depressors | |
| Design of the Movable and Fixed Control Components for the Consolidated Edison Thorium Reactor (Report BAW-147) | K-5A3 |
| 2.2 - THERMAL AND HYDRAULIC DESIGN | |
| 2.2.1 General Design Data | |
| Thermal and Hydraulic Design of the Consolidated Edison Thorium Reactor (Report BAW-132) | K-5A4 |
| 2.2.2 Design Methods and Correlations | |
| Thermal and Hydraulic Design of the Consolidated Edison Thorium Reactor (Report BAW-132) | K-5A4 |
| Irradiation Test Program for the Consolidated Edison Thorium Reactor (Report BAW-134) | K-5A5 |

# CONTENTS

## CONTENTS (CONT'D)

## LIST OF FIGURES

# I. INTRODUCTION

## A. GENERAL DESCRIPTION

The reactor core for the Consolidated Edison Thorium Reactor (CETR) contains 120 fuel elements. Each element is 137.50 inches long and 5.711 inches square. A cross section of the element is shown in Figure 1 and an over-all view in Figure 2. The fuel element assembly consists of a fuel bundle assembly, a fuel can assembly, an upper transition, a fuel element spring, and an upper nozzle and seal assembly.

The fuel is in the form of high density oxide pellets of close dimensional tolerance, contained in tubing made of a modified Type 304 stainless steel containing a small percentage of boron. Each tube is closed at the ends with suitable end caps. These are protected from excessive thermal stress by spacers at each end. The annulus between the pellets and the tubing is filled with helium. Each bundle (subassembly of tubes) contains 195 tubes, spaced by ferrules (short, thin, tubular sections) in a 14 x 14 square array with one corner tube omitted. The ferrules are spaced axially 9 inches center-to-center in planes perpendicular to the longitudinal axis of the bundle. A row of smaller ferrules is spaced around the outside of the bundle at each plane of ferrules to support the outer row of tubes, and to separate the fuel tubes from the can wall. The entire bundle is brazed as a unit.

Coolant flow control, flow distribution, and structural support for individual elements are provided by fuel element can assemblies. The fuel element can is made of Zircaloy-2 in the form of an envelope surrounding the tube bundle and is fitted at each end with transition pieces. A spring in each fuel element, locked in place by the top transition piece assembly, holds down the fuel bundle against hydraulic forces, while permitting thermal expansion of the bundles.

Each fuel element contains fuel of various uranium to thorium ratios, distributed through the core in a manner which will reduce power peaking.

The loading pattern chosen is a radial zone loading system and requires specific fuel bundle orientation. The core is divided into three radial zones. Fuel elements for Zone I (inner) have the lowest $UO_2$ concentration and fuel elements for Zone III (outer) have the highest $UO_2$ concentration. Figure 3 illustrates this loading arrangement.

Positive fuel bundle orientation is accomplished as follows. The missing corner tube on the bundle and an index strip in one corner of the can insure proper rotational orientation within the can. Two flow blocks attached to each element permit only the correct can orientation when placing elements in the core. If the can is incorrectly oriented, the flow blocks interfere with control rods or other parts of the core, preventing further assembly until the can is oriented properly.

## B. DESIGN REQUIREMENTS

The main function of the fuel element is to generate heat for the power plant. It is designed to fulfill the following requirements.

1. Maintain uniform spacing of fuel within the core.
2. Direct coolant flow for uniform cooling of the fuel rods.
3. Provide protection for the fuel rods against the effects of hydraulic loads and thermal expansion.
4. Provide a safe and reliable means for refueling the reactor.
5. Provide space for insertion of startup sources and proper channels for reliable operation of control rods.

# II. FUEL ROD DESIGN AND ASSEMBLY

## A. GENERAL

The fuel rod assembly consists of the following components; fuel pellets, fuel cladding in the form of a container tube, a lower end cap, fuel spacers, and a top end cap. The void space around fuel pellets inside the cladding tube is filled with welding grade helium.

The fuel rod assembly has the following functions.

1. It maintains the fuel distribution and spatial configuration required by the core design.
2. It prevents contamination of the fuel pellets from exterior sources.
3. It prevents contamination of the power plant with radioactive matter from the fuel and contains the evolved fission gases.
4. It provides efficient means for heat transfer from the fuel to the coolant.

## B. FUEL PELLETS

### 1. Description

The high density oxide pellets are composed of various mixtures of uranium oxide and thorium oxide.

The fuel pellets are divided into six categories. Five are composed of $ThO_2$ powder having different concentrations of $UO_2$, and are stamped with letter A, B, C, D, or E to designate an increasing degree of enrichment. The sixth type of pellet is composed completely of $ThO_2$ and is not stamped. The pellet identification letter is stamped on one end of the pellet as the pellet is formed in the die assembly. The density of the pellet mixture ($ThO_2 + UO_2$) is nominally 9.13 g/cc minimum (91% of the theoretical density of $ThO_2$).

Heat transfer parameters require a maximum gap of 0.004 inch between fuel pellets and the cladding. This requirement and the

minimum gap for assembly clearance requirements and the tolerance on the inside diameter of the cladding set the pellet diameter. The length to diameter ratio of individual pellets is approximately 3 and is established by optimum fabrication processes.

The condition and quality of the fuel pellets are of critical importance in the proper operation of the reactor. Inspection at various stages of manufacture starting with the powder analysis insures that strict quality control standards are met. Strict accountability of fissionable material is maintained.

2. Fabrication and Inspection

The fabrication of fuel pellets is rigidly controlled. Fabrication procedures control the fuel from the procurement of the $UO_2$ and $ThO_2$ powder to the loading of fuel pellets into the fuel rods. Inspection checks are made at various stages in the procedure to ensure that minimum requirements are met. The sequence of inspection and major steps in the manufacture of the fuel pellets are as follows.

1. Material received and certification checked for conformance to specification requirements.
2. Proper amounts of $ThO_2$ and $UO_2$ weighed in accordance with $UO_2$ concentration requirements and criticality limits.
3. Ball mill charges of oxide inspected on a sampling basis for percent uranium and homogeneity.
4. Oxide mixed in a ball mill and discharged into batches of equal weight in accordance with criticality limits. Three samples (minimum) extracted for chemical analysis.
5. Binders mixed in, mixture granulated and dried, lubricant blended in.
6. Pellets pressed to the specified green density for the particular powder lot and the batch weight recorded.
7. Pellets sintered to final density and the batch weight recorded.
8. Sintered pellets analyzed on a sampling basis for percent uranium, iron, and carbon.
9. Sintered pellets inspected on a sampling basis for minimum allowable density.

10. Open porosity determined on a sampling basis.

11. Pellets ground to final diameter.

12. Final inspection performed and pellets stored.

The pellet density is determined by weight and dimension, and inspection assures a 95/95 confidence level (95% assurance that 95% of the parts meet requirements). The open porosity is determined for the total core with a 95/95 confidence level by the procedure outlined in ASTM-C-373-55T, "Water Absorption, Bulk Density, Apparent Porosity and Apparent Specific Gravity of Fired Whiteware Products". Each major manufacturing step is completed for a given $UO_2$ concentration before processing the next lot to avoid mixing fuel pellets or materials of different enrichments.

## C. FUEL CLADDING

### 1. Description

The fuel cladding consists of a tube which is fabricated from modified Type 304 stainless steel containing boron. The tubing has the following finished dimensions.

Outside diameter — $0.304 \pm 0.0005$ inch

Inside diameter — $0.263 \pm 0.0005$ inch

Local wall thickness variations — $\pm 5\%$ of average wall thickness (due to eccentricity)

Length — $102.000 \begin{smallmatrix} +0.094 \\ -0.000 \end{smallmatrix}$ inches

Straightness — 0.005 inch per foot

The cladding material is required to contain the fuel and the radioactive fission products throughout the life of the element, and very stringent quality requirements are placed on the raw material. The material used for the cladding conforms to all of the requirements of ASTM A-213-57T TP 304 with the exceptions and amendments listed below.

a. No additions of "grain refiners" or rare earths shall be made.

b. Natural boron shall be added as an alloying agent to the basic material. The boron analysis of the finished tubing shall be $250 \text{ ppm} \pm 100 \text{ ppm}$.

c. Tubes shall be made by the seamless process.

d. Tubes shall be pickled to remove scale and passivated.

e. Throughout the manufacturing process, care shall be taken to thoroughly clean the tubing of residual contamination, prior to each heat treatment. Cleaning shall be performed in non-chloride bearing cleaning solutions or in a non-chloride molten salt bath below 1000 F. After cleaning, the tubes shall be rinsed with clean water to flush out residual cleaning agents.

f. An analysis for trace elements shall be run on the finished tubing for record purposes.

g. The tubing shall have a surface finish of 125 rms or better. The inside surface shall be clean and free from scale.

h. The tubing before acceptance must undergo a 100% eddy current test, a 100% surface penetrant test, and one hardness test per lot which will indicate on the Rockwell "B" scale, a hardness of 20 maximum.*

2. Wall Thickness Determination

The fuel rods are subjected to external pressure from the coolant during operation and the cladding wall thickness is based primarily on resistance to collapse. The effects of the external pressure are a maximum at the beginning of core life and gradually diminish as fission gas release provides a countering internal pressure and irradiation strengthens the cladding The cladding is free standing and requires no support from the fuel. The critical design area is the hot spot which has an average temperature of about 650 F and is subject to a thermal gradient of about 73 F.

The thickness of the cladding required to resist the external pressure only has been calculated, and has been confirmed by tests (see Appendix A). The results show that cladding with a minimum thickness of 0.019 inch has a margin against collapse of 19% above the 1800 psig design pressure neglecting the thermal gradient. Calculations indicate the thermal gradient at the hot spot has a weakening effect equivalent to thinning the cladding 0.0007 inch, which reduces the margin

* Lot as defined in ASTM A-213-57T.

against collapse to 15%. The minimum thickness of 0.019 inch plus tolerances becomes a nominal thickness of 0.0205 inch.

The 15% margin for the worst rod is considered more than adequate. All other rods have even more margin.

3. Axial Loading

The peripheral fuel rods are loaded as short columns by the weight of the fuel bundle and by the fuel element holddown spring force. Such short columns are generally stress limited and therefore sensitive to any eccentricity of loading which produces bending stresses in the fuel rods.

For this reason the shelves on the transition pieces, and the fuel rods and bundles are designed so the eccentricity of loading will be zero, or so small that no appreciable bending stresses will result under the most adverse combination of tolerances and clearances. The axial stress in the overhung ends of the peripheral fuel rods is simple compression, and is less than 14,000 psi under the worst conditions. Elsewhere, the stress is lower. For such short columns the limiting stress is the yield strength — about 17,000 psi.

4. Thermal Stress and Distortion

Differential thermal expansion between fuel rods may produce column loads in the rods between ferrules and cause the rods to bow excessively. The amount of bow caused by thermal differentials is dependent on the load, the initial bow, and the distance between supporting ferrules. Axial ferrule spacing and the permissible manufactured bow have been set so the operating thermal bow at any time during the core life will not excessively reduce the coolant channels or cause the rods to touch each other. The maximum operating thermal bow during the core life will not exceed 30 mils (refer to Appendix C).

The predicted and allowable bows discussed in Appendix C are based on an axial ferrule spacing of 8 1/16 inches for the reference bundle and the test bundle. After the testing was completed, ferrule spacing for the production bundles was set at 9 1/32 inches. Bow increase due to a length increase in the load range of interest is proportional to the square of the increase in length. The maximum

operating thermal bow in this case is increased from 24 to not more than 30 mils. Based upon extremely pessimistic assumptions, the maximum allowable bow for the 9 1/32-inch span is 33 mils providing a minimum margin of safety of 10%.

5. Effects of Hydrotest

The fuel cladding will not collapse during a hydrotest at 2700 psi external pressure and 140 F (see Appendix A).

D. END CAPS

1. General

The end caps are made of stainless steel to comply with ASTM A-240-58T TP 304, or A167-58 grade 3; and the chemical composition shall comply with ASTM A-371-53T, class ER 308. The end caps are cup shaped with an OD of $0.264 \begin{smallmatrix} +0.001 \\ -0.000 \end{smallmatrix}$ inch and a wall thickness of 0.025 inch. Each end cap is subjected to surface penetrant examination on its convex surface prior to assembly.

During assembly of the fuel rod, the end caps are pressed into both ends of the clad tubing and welded. Automatic welding equipment is used to provide consistent, satisfactory welds. The integrity of the weld and the external end cap surface is assured by visual inspection, 100% helium leak test, 100% surface penetrant examination, and sample destructive metallographic inspection.

2. Design Analysis

a. Internal Pressure

Calculations indicate the end caps as well as the fuel rods will withstand internal pressures in excess of 7000 psi at 650 F. This internal pressure is well above any value expected during the core life. The calculations performed are based on standard theory and have been confirmed by tests performed for another contract.

b. Transient Conditions

Transient temperature and pressure differences acting on the end cap during reactor operation are more severe than the steady state temperatures and pressure differences. Tests have been performed

to determine the effects of temperature and pressure cycling on the end cap closure (see Appendix E). These tests used temperature and pressure cycles more severe than the transients expected during reactor operation. No failures or indications of leakage were observed after testing and the end cap closure is satisfactory for reactor operating conditions.

## E. FUEL SPACERS

### 1. General

The fuel spacer is a disc with a hole drilled normal to the flat surface to provide a vent between adjacent fuel compartments, and an annular groove around the outside diameter to provide for locating the spacer within the fuel clad prior to brazing. It is made of AISI 304 stainless steel, and is Kanigen plated. The Kanigen plating is a brazing alloy which bonds the spacer to the cladding during the fuel bundle braze cycle.

The function of the spacers is two fold. It divides the fuel rod column into six equal length compartments with intermittent axial void spacers, and acts as a thermal insulator for the end caps.

## F. FABRICATION AND INSPECTION

The cladding tubing is cleaned by the tubing manufacturer and wrapped in paper. No further cleaning is employed unless required by inspection. The end caps and fuel spacers are inspected and processed by the following cleaning procedure:

1. Immerse in and wash with a hot solution of Alconox.*
2. Rinse in Grade A water.**
3. Immerse in acetone or alcohol.
4. Allow solvent to drain, and dry by shaking of filtered air blast.

After cleaning, all parts are wrapped in paper or plastic, and are handled with lint free gloves. After the final end closure of the fuel rod assembly is made, the assembly may be handled without gloves, if necessary.

* Wetting agent, Alconox Inc., New York 3, New York.
** Demineralized water with ph between 6 and 8 and resistivity of 500,000 ohms.

The assembling of the fuel rod is a carefully controlled procedure. The major steps in the procedure for the fabrication of the fuel rods are as follows:

1. Remove the paper covering on the cladding tubing and electroetch the serial number. The serial number identifies the individual tube and includes a letter to correspond with the fuel pellet type to be loaded into that particular tube. Its location also identifies the upper end of the fuel rod.
2. Random check the pellets for corresponding identification mark and arrange them in a loading tube to the specified length. Slight inherent differences in color between the different pellet types is another aid in checking pellets.
3. Record weight and length of fuel column for each rod.
4. Subdivide the fuel column into specified lengths for the compartments.
5. Load fuel spacers and short fuel columns into the clad. The cladding is crimped at each spacer. The spacer is located with respect to the individual fuel compartment to insure the minimum axial gap required for differential thermal expansion of fuel and cladding. Fuel rods are 100% inspected by X-ray and/or fluoroscope to insure that the spacer has been properly located.
6. A retort is used to evacuate the air from the fuel rod, and the rod is filled with helium. End caps are pressed into each end.
7. The end caps are welded to the cladding in an automatic welding fixture with an inert gas shield. The welds are cleaned with a stainless steel brush and the rods are wiped with alcohol or acetone saturated cloth.
8. After a visual inspection for cleanliness, all tube welds are leak tested with a helium leak detector. The detector is calibrated at least twice every eight hour shift against a standard leak. Tubes giving leak indication are rejected.
9. All end closure welds are visually inspected for evidence of folds, cracks and surface porosity.

10. The fuel rod assembly is washed in a hot solution of Turco, rinsed in hot demineralized water, and dried thoroughly.*

11. The exterior surface of each end cap and end cap weld is inspected by surface penetrant examination.

12. Each fuel rod assembly is color coded on the upper end as follows:

| | |
|---|---|
| Type A — Blue | Type E — Yellow |
| B — Green | F — Black |
| C — Red | |
| D — White | |

One sample weld is subjected to metallographic examination for every two hundred end cap welds. The test specimen is prepared from a longitudinal section. The depth of end cap weld penetration is measured with a microscope. The specimen is examined at 500X magnification for micro porosity and cracks.

Careful control insures that the fuel rod identification represents the type of pellets actually loaded into it. The fuel cladding and subsequent assemblies are completely segregated for each type of loading once the identification marking is applied. The individual rod serial numbers and corresponding pellet loading information are also recorded.

* Lye base cleaner, Turco 4182-A, Turco Inc., Los Angeles.

# III. FUEL BUNDLE DESIGN AND ASSEMBLY

## A. GENERAL

The fuel bundle consists of 195 fuel rod assemblies in a 14 x 14 square pattern (1 corner rod is omitted) and the necessary ferrules and sleeves to provide proper spacing and support for the rods. All of these individual parts are assembled in a jig during manufacture and then furnace brazed to form a single unit. The corner fuel rod is omitted to allow the fuel bundle to be oriented properly in the fuel element can assembly, and the fuel rod arrangement for each bundle is symmetrical about the diagonal through the missing fuel rod.

The parts required to produce a fuel bundle assembly include, in addition to the fuel rod assemblies, spacer ferrules, peripheral ferrules, and support sleeves.

## B. SPACER FERRULES

### 1. General

The spacer ferrules are made from Type 304 stainless steel tubing conforming to ASTM-A-213-58T, and are 0.225 inch OD x 0.018 inch wall. The spacer ferrules are located between fuel rods in planes 9 1/32 inches apart for the entire length of the fuel bundle. These ferrules space the fuel rods in a square array with a minimum resistance to the flow of coolant. The ferrules are 3/4 inch long except for those in the plane at each end of the fuel bundle, where 1 inch long ferrules are used to provide additional stability and strength.

The ferrules are Kanigen plated during manufacture. The Kanigen plating flows during the braze cycle and produces a brazed bond between the ferrules and the fuel rods.

### 2. Design Analysis

The principal load on the spacer ferrules during reactor operation is shear produced by differential thermal expansion of

adjacent fuel rods within a fuel bundle. The ferrules are made from material with a shear strength superior to the shear strength of the braze joint and have shear areas in excess of the minimum shear areas in the braze joints. The brazed joint strength is therefore the limiting factor for shear loads. (Brazed joint strength is discussed in Section III F.)

## C. PERIPHERAL FERRULES

### 1. General

The peripheral ferrules are made from Type 304 stainless steel tubing conforming to ASTM-A-213-58T, and are 0.123 inch OD x 0.015 inch wall. They are brazed with Nicrobraze 10 and are located in the same planes as the spacer ferrules, but they are on the periphery of the fuel bundle and supplement the spacer ferrules in supporting and spacing the fuel rods. A primary function of the peripheral ferrules is to insure a channel for coolant flow between the peripheral fuel rods and the fuel can; the ferrules project beyond the peripheral fuel rods for this purpose. The peripheral ferrules are 1/2 inch long except for those in the plane at each end of the fuel bundle. One inch long ferrules are used in the two end planes to provide additional stability and strength.

### 2. Design Analysis

Shear loads and conclusions identical to those discussed for spacer ferrules (Section III. B. 2.) pertain to the peripheral ferrules.

The peripheral fuel rods may also be subjected to radial loads in the unlikely event of interference between the fuel bundle and surrounding can (see Section III.H.). The small number of ferrules (10) required to carry the maximum load without yielding provides satisfactory assurance that the ferrules will not yield or allow the cladding to touch the fuel cans.

## D. SUPPORT SLEEVES

The support sleeves are 0.348 inch OD and are made from Type 304 stainless steel conforming to ASTM-A-213-58T. The sleeves are brazed (Nicrobraze 10) to each end of the peripheral fuel rods in a fuel

bundle to provide a means of supporting and locating the fuel bundle in the fuel can. The outer ends of the sleeves are machined after the fuel bundle is brazed to establish the surfaces which mate with the upper and lower transitions. The sleeves on the lower end are 15/32 inch long and are counterbored to fit over the fuel rod 1/4 inch. The sleeves at the upper end are 23/32 inch long and are counterbored to fit over the rod approximately the same amount. The added length on the upper sleeves is a machining allowance to compensate for variations in fuel rod length.

## E. FABRICATION AND INSPECTION

The major steps in the assembly and brazing of the fuel bundle are:

1. The support sleeves, spacer ferrules and peripheral ferrules are cleaned in a hot solution of Alconox, rinsed in Grade A water, immersed in acetone or alcohol, and dried. After cleaning, lint free gloves are worn by personnel during assembly of the bundle.
2. The fuel rods and ferrules are installed in a brazing fixture. Fuel rods with support sleeves are located on the periphery. The following precautions are taken during loading.
    a. All fuel rods are installed with the identification mark on the fuel rod at the upper end to insure uniform axial fuel location within the fuel bundle.
    b. A record is made of each fuel rod assembled in the bundle. Fuel rods are identified by serial number and color coding.
    c. Care is taken to ensure full contact between ferrules and fuel rods.
    d. Water channel spacers are installed between ferrule planes to support the fuel rods and minimize distortions during brazing.
    e. The peripheral ferrules and support sleeves are spot welded to the fuel rods to maintain proper position during brazing.
    f. The peripheral ferrules and support sleeve joints are coated with braze.

3. The fuel bundle is inspected before brazing for the following dimensions at a number of locations:

   a. Over fuel rods — $5.166 \begin{smallmatrix} +0.007 \\ -0.039 \end{smallmatrix}$ inches.

   b. Over peripheral ferrules — $5.196 \begin{smallmatrix} +0.003 \\ -0.059 \end{smallmatrix}$ inches.

   In the event that the bundle is out of tolerance, it must be restacked and reinspected.

4. A color coded template is placed against the upper end of the bundle to verify that proper fuel rod types have been used.

5. The upper end of the fuel bundle showing the color coded fuel rods is photographed with color film for record purposes.

6. The bundle is placed in the brazing furnace in an upright position. Thermocouples are attached to the upper, center, and lower portions of the bundle to record temperatures. Three test specimens are also placed in the furnace for subsequent examination to determine braze strength and to check the cladding for boron content after brazing.

7. The fuel bundle is identified by marking with a vibratool. The number is 3/16 inch high and is located on the upper end of the bundle on a support sleeve. Each bundle is marked with a zone number I, II, or III and serial numbers to run consecutively as follows: for Zone I — 1 through 32, Zone II — 33 through 76, and Zone III — 77 through 120.

8. A hydrogen atmosphere is used in the furnace until the furnace reaches a temperature of 1700 F; at this point the hydrogen is replaced with argon. This is done to avoid deboronization of the fuel rod cladding.

9. After brazing, the fuel bundle is checked to determine quality of brazing. The following standards apply.

   a. No loose spacer ferrules are permitted.

   b. On the end planes, every spacer ferrule must have a minimum of three good joints. The maximum number of unattached joints is limited to 10%. No missing spacer ferrules are permitted. Every fuel rod must have at least two good joints.

c. Peripheral ferrules must have two good joints. No two consecutive peripheral ferrules in any direction may be missing. If a peripheral ferrule is missing, the spacer ferrule joining the two affected fuel rods must have good joints with both rods.

d. Unattached joints may be repaired by applying braze material and recycling the bundle in the furnace. Test specimens from the first run are included in the recycling.

10. The completed assembly is subjected to a complete dimensional inspection. The more significant of these inspections are as follows:

    a. The external surfaces must pass through a reference envelope without interference. This envelope insures that accumulation of tolerances will not interfere with the proper location and installation within the fuel element can. The reference envelope is perfectly square and free of twist and measures 5.238 ± 0.000 inches square.

    b. The space between adjacent fuel rods is inspected at three points between ferrules to insure the minimum required fuel rod spacing.

11. Both ends (support sleeves) of the fuel bundle are machined to give an over-all length of 102.5 ± 0.030 inches.

12. The completed assembly is cleaned to assure a surface contamination level not exceeding 4.6 micrograms of U-235 per square foot and 75 micrograms of $ThO_2$ per square foot.

13. Before final acceptance of the fuel bundle, the following tests are made on the test specimens included in the brazing furnace:

    a. A tensile test and a braze examination are made to verify proper brazing.

    b. A chemical analysis is made to determine the amount of deboronization in the fuel rod cladding.

## F. BRAZED JOINT ANALYSIS

The individual fuel rods are restrained from relative axial movement by the ferrule-to-fuel-rod braze joints. These rods are

exposed to axial thermal expansion loads during operation resulting from thermal differentials between fuel rods. The maximum load is on the braze joints holding a corner rod which is 96 F colder than the surrounding rods.

An extensive test program on behalf of this and other reactor contracts has established that the braze joints produced by the specified production cycle and technique are more than adequate for this application (see Appendix B).

In the reactor the maximum loading (255 pounds per inch) occurs if the minimum allowable total brazed joint length ( 1 inch ) occurs on a corner rod which has the maximum load of 255 pounds. The minimum allowable strength of the brazed joints (as indicated by the pull test specimens brazed with each fuel bundle) has a 2.5:1 margin over this maximum loading.

In the testing summarized in Appendix B, overload factors of 1.97:1 and 2.72:1 produced practically no failures in the brazed joints, indicating that a margin greater than 2.5:1 exists in these joints.

## G. VIBRATION STUDY

The fuel rods may vibrate as beams between ferrule support planes due to coolant excitation during reactor operation. Tests were performed to determine if such vibration would result in fuel rod or ferrule fatigue failure.

The maximum expected vibratory amplitudes were determined to be well below those amplitudes which were demonstrated as necessary to produce fatigue failure in the cladding. The magnification ratio (ratio of dynamic to static deflection for the same loading) of a fuel rod was determined to be of the order of 1.4 to 2.0 and the rod is expected to be indifferent even to resonant excitation (see Appendix D).

## H. THERMAL DISTORTION STUDY

Fuel elements on the periphery of the reactor core are subject to a non-uniform flux distribution and thermal gradients up to about 50 F are produced across the fuel bundle. The thermal gradients cause the fuel bundle to bow as much as 0.090 inch toward the center of the core and combined with the worst tolerance conditions determine

the maximum possible interference between the bundle assembly and the can. The maximum possible interference of the bundle and the fuel cans is about 0.076 inch. The peripheral ferrules (which project beyond the fuel cladding) touch the can wall but the fuel cladding (because of its specified straightness) does not touch.

The 0.076 inch interference causes a load of about 220 pounds between the peripheral ferrules and the can, and a minimum of 10 ferrules is required to support this load without yielding. Assuming the contact occurs at two ferrule planes, 24 ferrules are available to support the load and there is little possibility that any ferrule will be overloaded. The fuel can is much stiffer than the bundle and will be deflected only about 0.010 inches in the worst case.

# IV. FUEL CAN DESIGN AND ASSEMBLY

## A. GENERAL

The fuel can assembly, which represents a major subassembly of the fuel element assembly, is composed of the following parts: fuel can, lower transition assembly, transition attachment screws, flow blocks, and index strip. (See Fig. 2.)

The primary functions of the fuel can assembly are:

1. Furnishes mechanical support for the fuel bundle, upper transition, spring, and upper nozzle seal assembly.
2. Provides separation of coolant flow between the fuel bundle and the control rod channels.
3. Provides efficient entrance and exit of the coolant flow into and out of the fuel bundle.
4. Establishes the proper location of the fuel element within the core.
5. Provides the means for safe handling and positive indexing of the fuel bundle.

## B. FUEL CAN

### 1. Description

The fuel can is a square tube with a wall thickness of 0.155 inch, an inside dimension of 5.401 inches, and a length of 117 5/16 inches. It is made from reactor grade Zircaloy-2 for Class II application as specified by MIL-Z-19859A. The fuel can is fabricated from plate stock and the major steps in the manufacturing procedure are:

a. Plate stock is heated and bent into channels.

b. The outside and inside radii of all formed angles are checked for cracks, slivers, scales, blisters, seams, folds, and foreign matter by visual inspection.

c. The outside radii of all angles are 100% inspected by the dye penetrant method. Any defect which cannot be polished out without exceeding the drawing tolerances is cause for rejection.

d. Two channels are welded together full length to form a fuel can. The welding is performed in a helium atmosphere using automatic welding equipment.

e. Rough weld surfaces are ground smooth and cleaned of all contamination. The welds are then 100% inspected by dye penetrant methods.

f. The welded assembly is vacuum annealed for a minimum of one hour at 500 F and one micron vacuum.

g. Both ends of the can, and the bayonet slots at the top, are machined.

h. Each completed fuel can is corrosion tested for three days in 680 F water. The water used must have a pH of 7 ± 1, a minimum resistivity of 500,000 ohm - cm, and a maximum oxygen content of 0.03 cc/kg. No gross corrosion in excess of 5% of the surface area is allowed.

i. A serial number, with letters and/or numbers 1/4 inch high and 1/64 inch deep, is engraved on the upper end of the fuel can with a vibratool for identification purposes. The number identifies the individual fuel element assembly and includes a zone designation.

j. The fuel can is checked dimensionally against a theoretical envelope which is perfectly square and free from bow and twist. The can may have any combination of distortions, limited by the tolerances on the detail drawings, provided it will pass through the inspection envelope. It must also be possible to pass an internal inspection mandrel through the can without interference or binding. The internal mandrel is 5.359 ± 0.005 inches square x 77 inches long. The inside dimensional limitations insure the required clearance and spacing for the fuel rod bundle. The outside dimensional limitations insure the necessary space between fuel element cans for installation in the reactor, and provide the necessary clearance for control-follower rod assemblies and other control elements.

   An end plug gage, 5.3900 ± 0.0005 inches square, must enter each end of the can for a distance of 4 inches. The ends of the can must be parallel within ±0.010 inch and perpendicular to the can centerline within ±0.005 inch total indicator reading. These dimensional limitations are necessary to provide for insertion of the upper

and lower transitions and to limit coolant by-pass leakage to or from the control rod channels.

2. Design Analysis

Fuel can bending stresses due to pressure are determined by beam analysis assuming built-in ends at the corners. Beam loads are uniformly distributed and derived from the differential pressure across the can wall. The differential pressure across the can wall varies from a maximum 17 psi internal pressure to a maximum 17 psi external pressure in approximately a linear gradient from the bottom to the top of the fuel bundle. Rivet attachments are located away from the ends of the fuel bundle to take advantage of the reduced pressure differential towards the center of the can.

Corner stresses are corrected for stress concentration according to curved beam analysis, and the stresses at the corners where rivet holes occur, are further modified with stress concentration factors for holes in plates in plane bending. The midspan stress at the can wall longitudinal weld is determined using the minimum wall thickness allowed after weld undercutting and corrected for the resultant notch concentration. All of the stress values listed herein include applicable stress concentration factors.

The maximum stress in the can corners at the top and bottom of the fuel bundle is about 13,000 psi. At the same vertical location, the maximum stress at the weld at the midspan of the can wall is 19,000 psi using an assumed notch radius of 0.005 inch. The minimum notch radius will probably be more nearly 0.020 inch, instead of the 0.005 inch assumed, since the weld undercutting is a concave meniscus type of surface from melting of the base metal. The larger radius gives a stress concentration of 2.0 instead of 2.87 and a midspan weld stress of about 13,500 psi.

The maximum stress at the hole for the upper rivet attaching the flow block is about 13,000 psi. The highest corner stress of 22,000 psi occurs at the hole for the lower rivet attaching the corner index strip. All other areas of attachment for the various components have stresses lower than these.

The maximum allowable design stress in the zones of stress concentration is set at 23,000 psi which is about twice the proportional limit of the material at operating temperature. This stress level is allowed because there is no reversed bending of the can walls. Some local yielding may occur in the concentrated stress regions at initial pressurizing but further stresses due to load changes, shutdown, and startup will not cause additional yielding. (Usually stresses produced by this type of loading may safely equal twice the yield strength of the material; a lower limit is specified here because of experience with low ductility observed in Zircaloy-2 in some instances.)

Nominal stresses not affected by stress concentration factors are acceptable up to a value of 15,000 psi, the yield strength of the material. All of the nominal stresses (without concentration factors) due to pressure effects on the fuel can are in a range of 5,000 to 11,000 psi.

## C. LOWER TRANSITION ASSEMBLY

The lower transition assembly is a weldment consisting of the lower transition casting and the lower transition tube. The casting used for the upper portion of the transition basically complies with the requirements of Grade CF8 of ASTM A351-57T with the following modifications.

1. The cobalt content will be 0.20% maximum. The analysis is to be recorded on a certified test report.
2. The castings shall be liquid penetrant examined over 100% of their surfaces.

The lower transition tube is made from Type 304 stainless steel, is 4 inches OD by 0.375 inch wall thickness, and is 13 3/16 inches long.

The lower transition assembly forms the lower portion of the fuel can assembly and has a total length of 18 3/4 inches. A 5.370 inch square cross section at the top end mates with the inside of the can and a square flange acts as a limit stop to position the casting within the fuel can at final assembly. The square cross section below the flange mates with pins projecting from the grid plate and establishes

the radial orientation of the fuel elements. The conical surface below the square cross section of the casting provides a seating surface to mate with the lower grid plate. The lower end of the tube for a distance of 4 inches is chrome plated to a finished diameter of $3.745^{+0.000}_{-0.005}$ inches. This diameter and the conical seat locate the fuel element in the lower grid plate. The extreme lower end of the tube is tapered for a distance of 1 inch to facilitate insertion into the lower grid plate. The upper end face of the transition provides a surface to locate and support the fuel bundle assembly. The transition assembly is designed for minimum resistance to flow of coolant from the lower grid plate to the fuel bundle.

## D. TRANSITION ATTACHMENT SCREW

Four special screws fabricated of Type 304 stainless steel are used to attach the lower transition assembly to the fuel can. The screws are threaded into the transition through each side of the fuel can. The head of the screw extends through a close fitting hole in the fuel can and is locked in place with a lock pin through the screw head into the transition. The screw head is 3/4 inch in diameter and four of them will support, in shear, the weight of the fuel bundle, lower transition assembly, upper transition piece, and the load imposed by the fuel element spring.

## E. FLOW BLOCKS

The flow blocks are rectangular strips, 3/8 inch x 1 inch x 99 3/8 inches long. The strips are made of Zircaloy-2 material to the same specifications as for the fuel can. Flow blocks are attached to two corners of the fuel element can with flush stainless steel fasteners and almost span the entire active fuel length. The blocks are located on the cans to occupy the gap between fuel cans in the reactor, immediately outboard of the control-follower rod cruciform tips. The lower ends of the blocks are chamfered to avoid "hang-up" during installation of fuel elements in the reactor.

The primary function of the flow blocks is to assure proper coolant flow distribution in individual control rod channels. This is accomplished by eliminating the open flow area that would otherwise exist. Other significant functions are:

1. The blocks displace the moderator to reduce flux peaking in an area that cannot be occupied by the control-follower rod assembly.
2. The blocks provide a visual indication, and an interference member, to avoid improper radial orientation of the fuel element assembly in the reactor.
3. The top surface of the flow block is machined to a different configuration for each zone providing a means to visually identify fuel elements of each type in the reactor.
4. Four Zone 1 fuel elements have modified flow blocks to provide a receptacle, 1/4 inch square and 66 inches deep, for start-up sources. A slot is cut from the top on one of the flow blocks of each of these four fuel elements and is covered by welding a full length strip flush with the face of the block.

## F. INDEX STRIP

The index strip is a triangular strip made from Zircaloy-2 to the same material specification as for the fuel can. The index strip is made in three sections having a combined length of 87 15/16 inches and is attached to one inside corner of the fuel can with flush stainless steel fasteners. The missing corner fuel rod on the fuel bundle and the index strip in the fuel can insures proper radial orientation of the fuel bundle within the fuel can.

## G. FABRICATION AND INSPECTION

The assembling of parts to complete a fuel can assembly is primarily that of mechanical attachment. Close dimensional control and inspection of the individual parts result in a minimum of such control and inspection during assembly.

The major assembly steps are as follows:

1. Locate and attach the index strip to the fuel can.
2. Locate and attach the flow blocks to the fuel can.
3. A template is used to check proper relationship of the flow blocks to the index strip.

4. The spaces between the fuel can sides and the mating transition surfaces are measured to obtain the proper location of the lower transition assembly. The transition is positioned to equalize these spaces and is held in position. The threaded holes and counterbores for the special attachment screws are machined in this assembled position. The counterbores are reamed to affect a "dowel fit" with the special screw head.
5. The special screws are installed and secured with the locking pins.
6. A final dimensional inspection of the assembled components is performed and the fuel can assembly is then ready for installation as a subassembly of a fuel element assembly.

# V. FUEL ELEMENT DESIGN AND ASSEMBLY

## A. GENERAL

The fuel bundle and fuel can assemblies have been discussed in previous sections. The remaining components of the fuel element and the final assembly and inspection procedures are discussed in the following paragraphs. The assembled fuel element is shown in Figure 2.

## B. UPPER TRANSITION

The upper transition mates with the fuel bundle, the upper nozzle seal assembly and the fuel element spring. The transition is 11 7/16 inches long and a 5.340 inch square cross section at the bottom mates with the fuel bundle. A 3.738 inch diameter at the top mates with the bore of the nozzle seal assembly and a flange provides a seat for the fuel element spring. The mating surfaces for the nozzle seal and spring are electro-filmed to prevent galling of the base material. The mating diameter with the nozzle seal is spherical and provides alignment of the telescoping surfaces without binding.

The transition is designed for a minimum resistance to flow of coolant from the fuel bundle to the nozzle seal assembly. Type 304 stainless steel cast material is used for the transition. The casting basically complies with the requirements of Grade CF8 of ASTM A351-57T with the following modifications.

1. The cobalt content will be 0.20% maximum. The analysis is to be recorded on a certified test report.
2. The castings shall be liquid penetrant examined over 100% of their surfaces.

## C. FUEL ELEMENT SPRING

### 1. General

The fuel element spring is made from 0.625 inch diameter, Inconel "X" centerless ground rod, and has the following dimensions:

5 1/8 inches OD, 8.815 inches free length, and 5.460 inches solid length. The main functions of the fuel element spring are as follows:

a. It provides holddown loads on the fuel bundle to prevent hydraulic flow from raising the fuel bundle, at the same time providing holddown loads on the lower grid plate to counteract the hydraulic forces on that assembly.

b. It provides holddown loads on the fuel bundle within the fuel can to prevent movement of the bundle during handling of the complete assembly.

c. It allows differential thermal expansion of fuel elements and thermal shields to occur without damaging the fuel elements or other reactor internals.

### 2. Design Analysis

Two major load conditions are imposed on the fuel element spring. During fuel element assembly, the spring is momentarily compressed to almost solid height. The calculated stress at this condition is 64,300 psi. The design allowable torsional strength of the spring at room temperature is over 70,000 psi.

The other load condition for the spring is the holddown spring load at operating temperature. This load is a maximum of 800 pounds with the spring compressed to operating height. The stress at this load is 45,000 psi. At this stress level, no relaxation will occur in the spring. This stress also is well below acceptable yield stress levels.

## D. UPPER NOZZLE AND SEAL ASSEMBLY

### 1. General

The upper nozzle and seal assembly consists of the upper nozzle, seal, and four locking pins. The assembly is approximately 8 1/4 inches long. The lower section is the seal and is 5.380 inches square. The upper section is the nozzle and is primarily 4 1/2 inches diameter. All materials used in the assembly are Type 304 stainless steel. The nozzle and seal are made from castings which comply with the requirements of Grade CF8 of ASTM A351-57T with the following modifications:

1. The cobalt content is 0.20% maximum. The analysis is to be recorded on a certified test report.
2. Castings shall be liquid penetrant inspected over 100% of their surfaces.

The upper nozzle and seal assembly serves the following major functions:

1. Minimizes coolant leakage from the fuel element.
2. Provides a mating surface with the upper grid plate.
3. Provides a means of locking the fuel bundle in the fuel can.
4. Provides a means of grasping the fuel element for handling.
5. Provides a mating surface for the fuel element spring.

The nozzle is free to rotate in the seal and is held by four locking pins attached to the nozzle 90 degrees apart. The pins project through the wall of the seal when the nozzle is rotated so the pins are on the major axes. When the nozzle is rotated so the pins are 45 degrees from the major axes, the pins are in the corners of the square seal and do not project. The pins when projecting through the seal are in a position to engage bayonet type slots in the fuel element can.

The upper end of the nozzle locates in a hole in the upper grid plate. A spherical seat on the nozzle is provided to mate with the upper grid plate to accomodate angular misalignment. Notches in the upper end of the nozzle, and a step on the inside diameter, provide a means of grasping the nozzle for handling and assembly. The inside diameter at the lower end of the nozzle mates with the top of the upper transition. This surface, the spherical seat, and the largest outside diameter are chrome-plated for wear resistance. The lower face of the nozzle mates with the fuel element spring. This surface is electrolized to facilitate assembly and to avoid galling of the base material.

The seal is square to fit the inside of the fuel element can. A slot is provided on each side to allow the locking pin to project. The outside square surface and diametral mating surface for the nozzle are electro-filmed to avoid galling.

2. Design Analysis

The nozzle and seal assembly requires an applied axial force of 1200 pounds to compress the fuel element spring and engage the

bayonet lock with the fuel can assembly. Concurrent with the axial force, a torque of 70 to 100 feet-pounds is required to rotate the nozzle and lock the bayonet. The notches in the top of the nozzle are for application of a bar or lugs of a wrenching tool to apply this torque. The maximum permissible torque applied to the nozzle, assuming two notches working and an allowable bearing stress of 30,000 psi, is 250 feet-pounds. Stresses produced in the fuel can and other parts by this maximum torque are very low.

## E. FINAL ELEMENT ASSEMBLY

### 1. General

After assembly of the major subassemblies, the fuel element final assembly is accomplished in the following sequence:

a. The fuel can assembly is placed into the assembly fixture.

b. The fuel bundle assembly is inserted into the can.

c. The upper transition and fuel element spring are inserted into the can and placed on top of the bundle.

d. The nozzle seal assembly is inserted into the can with the four pins in the diagonal corners of the can. The nozzle seal assembly is then forced into the can against the fuel element spring until the pins are at the bottom of four "L" shaped slots in the can. At this point the nozzle is rotated 45 degrees and allowed to back off. During this phase of the assembly, the four pins slide up into the slots, which restrain the nozzle from rotation and disassembly.

### 2. Marking and Orientation

Special inspection precautions during assembly of the fuel bundle insure that fuel rods of various $UO_2$ concentration are properly located within the bundle. The fuel bundle assemblies are marked with serial number and zone number. Fuel can assemblies are also marked by serial number and zone number thus providing complete control of the identity of fuel components.

Index strips in the can assembly insure that the bundle is placed in the can in only one orientation. Flow blocks placed on the can in an assymetric pattern provide a visual index to the can orientation.

The flow block geometry also prevents installation of subsequent assemblies if an element is placed in the core in an incorrect orientation. Flow block ends have three different shapes to provide visual zone identification of the fuel elements.

These inspections and provisions insure that fuel rods are installed in their intended orientation and location within each fuel element, and within the core.

3. Cleaning and Shipping

Special cleaning processes are used for the fuel element components during final assembly. After assembly the elements are wrapped and sealed to maintain cleanliness during shipping and storage.

Specially designed shipping containers are used to avoid damage to the fuel elements during transit from the manufacturing facility to the reactor site.

## F. ALIGNMENT STUDY

Studies to determine the maximum misalignment of a fuel element, with the upper grid plate removed, were performed to insure adequate lead-in and to prevent damage to the fuel element during installation of the upper grid plate assembly. The misalignment data were also required by handling tool fabricators for the design of fuel element installation tools.

The radial motion of the upper fuel element nozzle was calculated to be 0.300 inch. The lead-in on the upper grid plate is adequate for 0.625 inch nozzle misalignment.

The distance between adjacent fuel bundles is also an important factor in the design of the reactor since it affects flux peaking factors. Calculations of maximum possible fuel bundle misalignment were performed to determine the possible variation in gap between adjacent fuel bundles.

The maximum variation in the gap between the peripheral fuel rods of adjacent fuel bundles is 0.205 inch in the upper end of the core. This is for the case where tolerances and clearances combine adversely to give the maximum change in gap, and is not great enough to cause excessive flux peaking in the fuel elements.

FIG. 1: FUEL ELEMENT CROSS SECTION

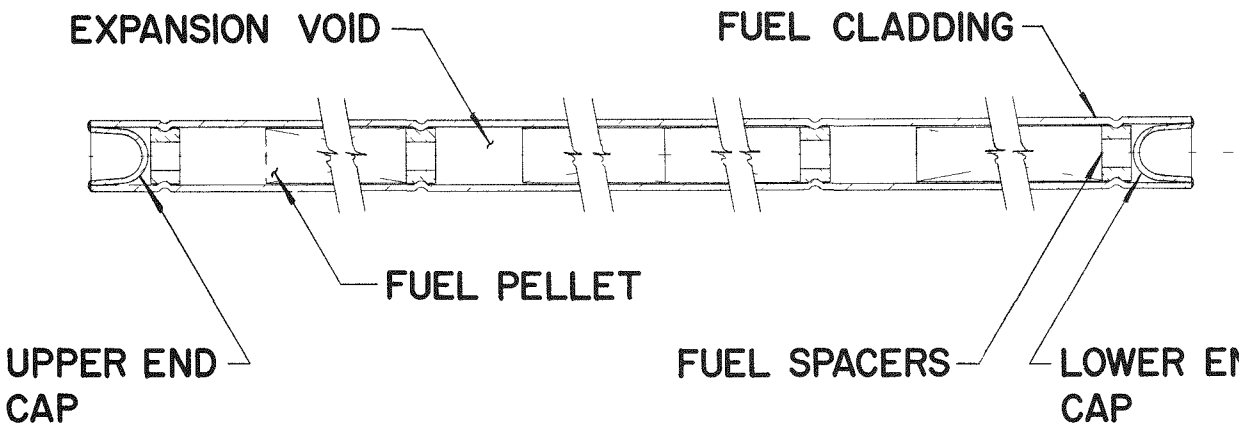


FUEL ROD DETAIL

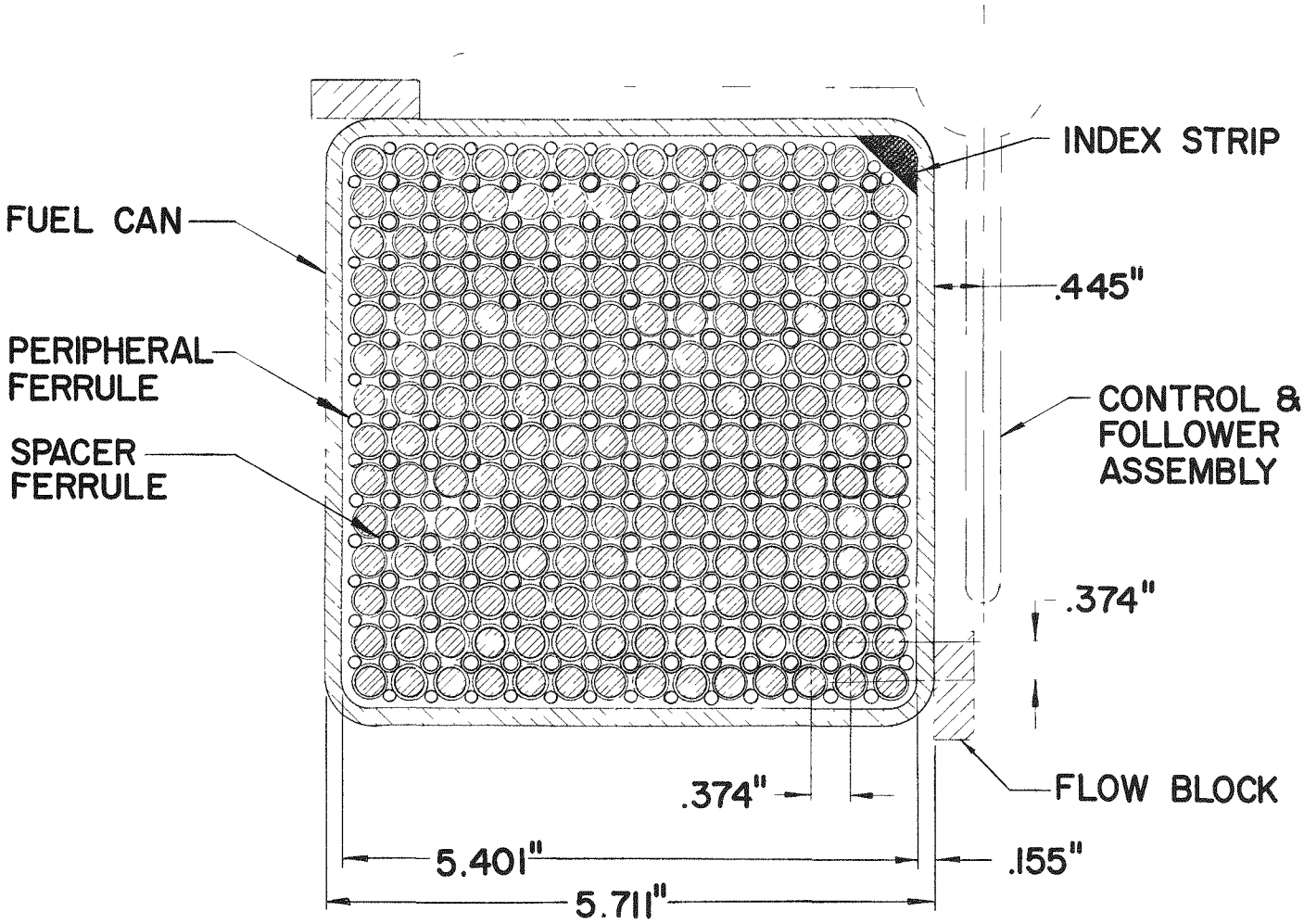

FIG. 2: FUEL ELEMENT

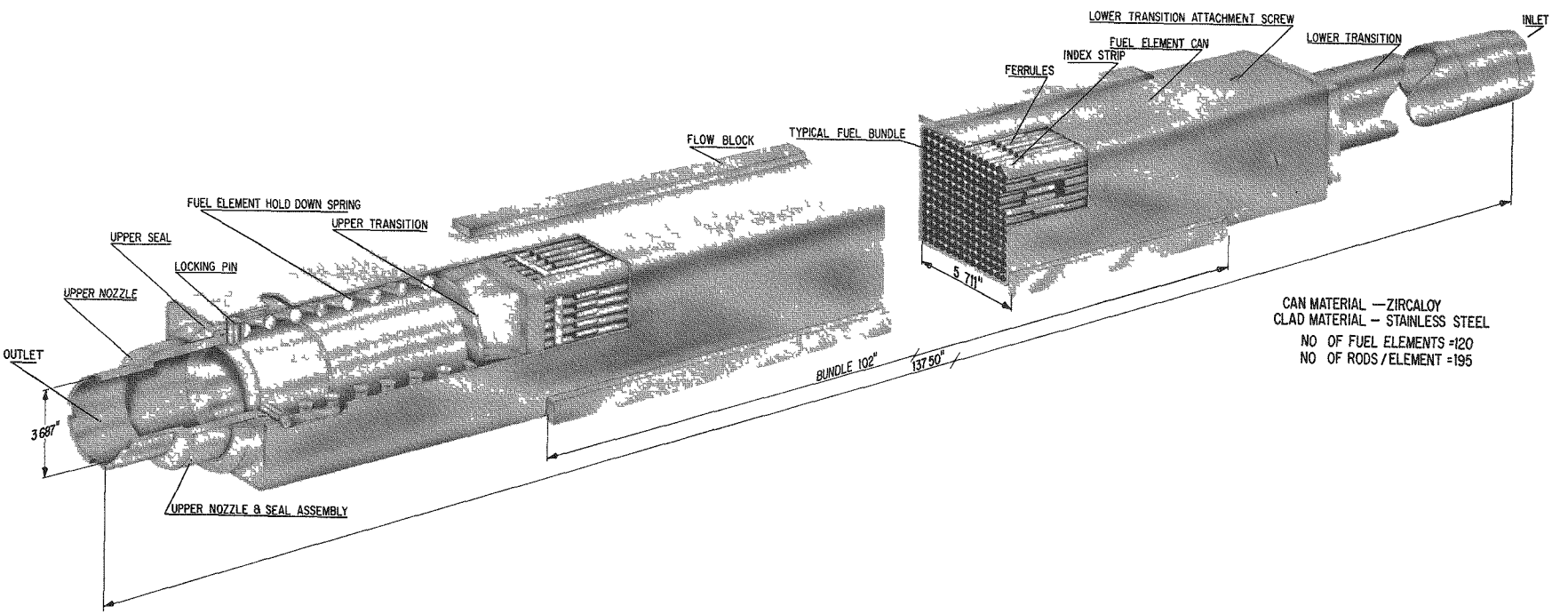

FIG. 3: CORE HARDWARE POSITION DESIGNATIONS

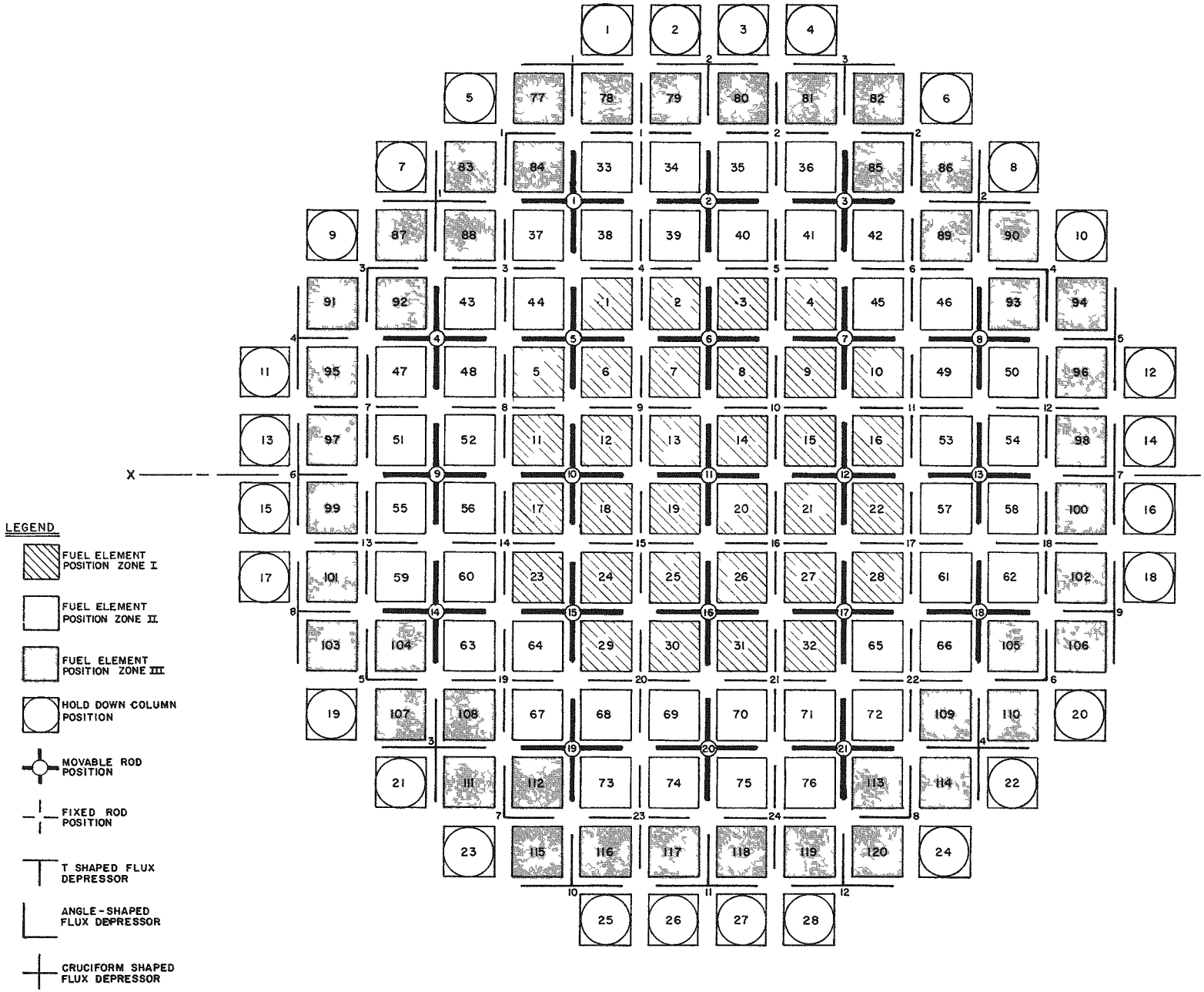

# FIG. 4: FUEL ELEMENT LOADING PATTERNS

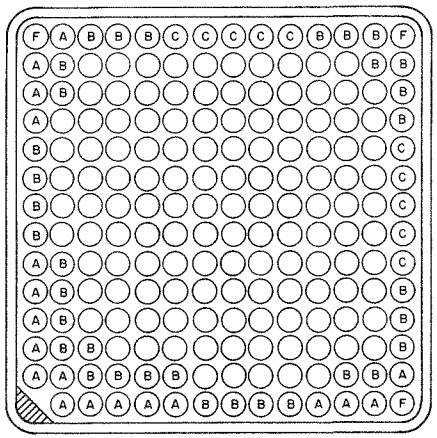

ZONE I

(ALL UNMARKED RODS ARE ENRICHMENT C)

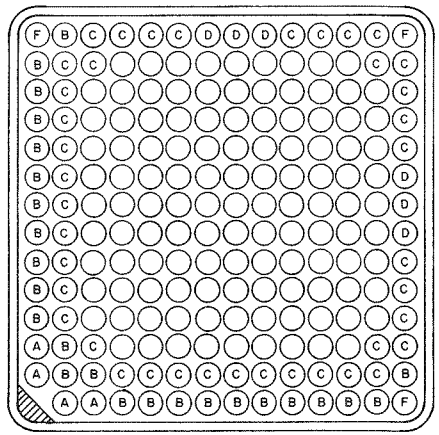

ZONE II

(ALL UNMARKED RODS ARE ENRICHMENT D)

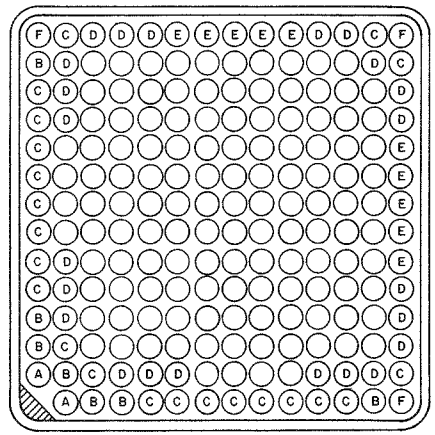

ZONE III

(ALL UNMARKED RODS ARE ENRICHMENT E)

LEGEND

A — LOWEST ENRICHMENT
B — SECOND LOWEST ENRICHMENT
C — THIRD " "
D — FOURTH " "
E — HIGHEST ENRICHMENT
F — 1/3 $ThO_2$ + 2/3 ENRICHMENT A

# VI. APPENDICES

# APPENDIX A
# COLLAPSE TEST SUMMARY

## 1. OBJECTIVES

A cladding thickness of 0.0205 inch for the CETR fuel rod was originally estimated from previous test experience. This preliminary estimate was required so nuclear, heat transfer, and flow calculations could be performed prior to completion of the testing. The testing covers two phases of confirmatory work. These phases are confirmatory testing performed on early groups of tubing during the design phase of this reactor and confirmatory work done on actual production tubing as soon as it became available. A further object of the testing is to determine the adequacy of the tubing under a cold hydrotest of 2700 psig at about 140 F.

## 2. CONCLUSIONS

A minimum clad thickness of 0.019 inch is adequate to resist the reactor design pressure of 1800 psig, and the hydrotest pressure of 2700 psig without collapsing. Tubing with 0.019 inch minimum wall thickness will not collapse below 2065 psig during reactor operation, nor below 3400 psig during hydrotest.

## 3. DESCRIPTION

All fuel rods were end capped prior to testing and subjected to the braze temperature cycle anticipated at that time for bundle production. A series of wall thickness and outside diameter measurements were taken to help evaluate the test results. Test specimens were placed in an autoclave at room and operating temperatures and pressurized until collapse occurred.

## 4. RESULTS

Table A-I shows the results of collapse testing on production tubing at 650 F and at room temperature.

Table A-II shows the results of collapse testing performed during the design phase of the reactor.

## 5. DISCUSSION

Previous testing experience indicated that a minimum clad thickness of 0.019 inch would give a minimum collapse margin of 6% over the design pressure. Design phase confirmatory testing with improved specimens (the tubing ID was not exposed to the brazing atmosphere — giving more realistic simulation of production conditions and possibly stronger material) indicated that during reactor operation no collapse would occur below 2065 psig (15% margin). Production tubing specimens indicated that no collapse would occur below 2325 psi (29% margin).

At that time it was not considered wise to take advantage of the high margin (15%) indicated by the design phase testing, because the production tubing might have lower strength. However, the production braze cycle (1 hour at 1800 F maximum) is less severe than that used on the design phase specimens. This combined with possibly higher strength gives the very high margins found on production tests. The above pressures are based on the calculated effective thickness loss of 0.7 mils due to the thermal gradient across the clad wall.

The production testing includes 3 specimens at reactor operating temperature and 3 specimens at room temperature. Good agreement is found between predicted collapse pressures (based on yield strength) and actual collapse pressures. The production test results give strong confirmation to the design phase testing.

Test collapse pressures are converted to reactor equivalent hot spot collapse pressures by correcting to minimum allowable wall thickness (0.019 in.), by reducing the clad thickness by 0.7 mils to account for the thermal gradient and by adding about 85 psi for differential internal pressure.

All temperatures and gradients are based on overpower, hot channel, flux peaking conditions; and represent the highest possible temperatures in the reactor. Thicknesses calculated are minimums. Tolerances must be added to get the nominal values.

TABLE A-I

RESULTS OF COLLAPSE TESTING ON PRODUCTION CLAD TUBING

| Test Temp, F | Collapse Pressure, psig | $t_{min}$, in. | Measured Yield Strength at Test Temp, psi | Theoretical* Yield Strength at Test Temp, psi | Equivalent Reactor Collapse - Hot Spot Pressure** (t = 0.019 in.), psig |
|---|---|---|---|---|---|
| 650 | 2575 | 0.020 | 19,100 | 19,600 | 2440 |
| 650 | 2450 | 0.020 | 19,100 | 18,700 | 2325 |
| 650 | 2510 | 0.020 | 19,100 | 19,100 | 2385 |
| 70 | 4800 | 0.020 | 28,600 | 36,500 | 3740 |
| 70 | 4375 | 0.020 | 28,300 | 33,300 | 3410 |
| 70 | 4475 | 0.020 | 29,200 | 34,000 | 3490 |

* Theory and experience indicate that the tubing will collapse when the average hoop stress equals the material yield strength.

that is, $S_{Hoop} = \frac{Pcr\ Ro}{t_{min}} = \frac{2575 \times 0.152}{0.020} = 19,600$ psi,

where Pcr = Test collapse pressure

Ro = Tubing outside radius

$t_{min}$ = Minimum clad thickness

$S_{Hoop}$ = Average hoop stress on minimum wall, and in this case, the theoretical yield strength.

** Includes maximum average clad temperature, minimum internal pressure and maximum thermal gradient across the clad thickness.

TABLE A-II

RESULTS OF COLLAPSE TESTING ON DESIGN PHASE TUBING

| Test Temp, F | Collapse Pressure, psig | $t_{min}$, in. | Measured Yield Strength at Test Temp, psi | Theoretical* Yield Strength at Test Temp, psi | Equivalent Reactor Collapse Hot Spot Pressure** (t = 0.019 in.), psig |
|---|---|---|---|---|---|
| 645 | 2300 | 0.0200 | ★ | 17,500 | 2185 |
| 648 | 2250 | 0.0198 | ★ | 17,300 | 2165 |
| 648 | 2400 | 0.0200 | ★ | 18,200 | 2285 |
| 647 | 2175 | 0.0201 | ★ | 16,500 | 2065 |
| 642 | 2230 | 0.0197 | 18,000 | 17,200 | 2155 |

* See Note on Table A-I.

★ Tensile specimens failed at end welds.

** Includes maximum average clad temperature, minimum internal pressure and maximum thermal gradient across the clad thickness.

# APPENDIX B
# BRAZE SHEAR STRENGTH TEST SUMMARY

## 1. OBJECTIVES

The objective of this test is to determine the shear strength of the ferrule to fuel rod braze joint material since it is not available for the required shape and temperature.

## 2. CONCLUSIONS

Kanigen braze joints are satisfactory to resist the maximum shear loads expected during reactor operation with a minimum safety margin of 2.

## 3. DESCRIPTION

Temperature differentials (greater than those expected under reactor operating conditions) were created between selected individual rods and the remaining rods of the test bundle which was half length but full cross section (see Appendix C for further bundle details). The temperature differentials caused adjacent rods to expand differently thereby applying a shear force to the braze joints. The effects of these shear loads were determined by sectioning the bundle after testing and examining the braze joints.

## 4. RESULTS

Table B-I shows results of bundle sectioning and Nicrobraz joint examination of tested rods after exposure to $\Delta T$ tests.

TABLE B-I

| | |
|---|---|
| Total number of joints tested and inspected | 1498 |
| % joints having partial braze | 5.9 |
| % cracked joints * | 5.3 |
| % porous joints | 0.4 |
| Total imperfect joints | 11.6% |
| Remaining (good) joints | 88.4% |

* These joints include any joints that show evidence of a crack; this includes surface cracks and complete fractures.

## 4. DISCUSSION

The room temperature bundle $\Delta T$ testing was performed before finalization of the production braze cycle, on a bundle having Nicrobraz joints Temperature differentials during bundle testing were higher than those expected for corner rods during reactor operation, and the room temperature rods are much stiffer than those in the reactor. These factors provide a margin of 1.97 on corner rods and 2.72 on other rods over operating temperature shear loads. A significant increase in the operating loads is not likely even if the calculated temperature differences should be in error by a large factor since the material (in the reactor) is working in the plastic range.

Results indicated that a high percentage of joints (see Table B-I) were still satisfactory after the $\Delta T$ test.

Production bundle manufacturing conditions were set as follows:

Braze material - Kanigen

Braze cycle - 1 hour at 1800 F

Testing performed on another reactor shows that there is no appreciable difference between good Kanigen and good Nicrobraz joints from the standpoint of strength. (See Appendix F.) However, Kanigen can be expected to provide a higher percentage of good joints. Backup braze strength testing on simple shear specimens (Kanigen brazed) also indicated that the production braze cycle did not alter the braze strength appreciably. In fact, this backup braze strength testing indicates a minimum margin of two and an average margin of 3.9 over the maximum shear load expected during reactor operation. Since practically no joint

failures resulted from an overload factor of nearly two (actually 1.97) in the bundle test, the backup testing confirms the results of the bundle test.

# APPENDIX C
# FUEL ROD BOW TEST SUMMARY

## 1. OBJECTIVES

The spacer ferrules joining the fuel rods are very stiff. Where a given rod is hotter than those adjacent to it, the hot rod is restrained from expanding completely in the axial direction. This results in a compressive, column type of load in the hotter rod. This column loading produces a bowing deflection of the rod between ferrule planes. The amount of bowing is dependent on the initial bow in the rod "as-manufactured", and the distance between ferrule planes which act as nodes. It is desired to determine what "as-manufactured" bow and ferrule plane spacing may be specified so the fuel rods will not deflect enough to excessively block the coolant flow channels, or touch each other.

The thermal differentials between rods may also distort the over-all bundle. It is desired to determine the degree of this distortion.

The analytical approaches available are not considered adequate to give sufficiently accurate results, for the reasons listed below.

1. The fuel rods are not elastic columns.
2. The end restraint is unknown.
3. The degree of eccentricity of load application is unknown.
4. The effects of reactor pressure are unknown.
5. The effects of long time exposure at temperature are unknown.

## 2. CONCLUSIONS

The operating thermal bow at any time during the core life will not exceed the allowable value of 0.027 inch, and therefore rods will not touch adjacent rods or excessively block the flow channels. The maximum bow will be less than 0.024 inch.

The existence of thermal differentials for short or long periods of time does not cause any appreciable change in the over-all dimensional

condition of the fuel bundle.

## 3. TEST DESCRIPTION

Four types of tests were performed.

1. High temperature, long time, bundle test to determine the effects of long time at temperature.
2. Room temperature, short time, bundle test to determine the effects of short time loading.
3. Broken ferrule test (a part of 2 above) to determine the effects of broken or unbrazed joints.
4. Autoclave column test on individual rods to determine if pressure at temperature has a harmful effect on deflection.

Two bundle specimens were used for the first three tests; one bundle for the high temperature test and one for the room temperature tests. Both specimens were cut from the same parent bundle. The bundle consisted of empty, 99 inch long, Type 304 stainless steel tubes, held together with Type 304 stainless steel ferrule spacers, in a 14 x 14 rod rectangular pattern.

For the reactor temperature bundle test, the initial fuel rod bow values between ferrule planes were measured and recorded at room temperature. The test specimen was then mounted vertically in a furnace The furnace was heated to reactor operating temperature (650 F), and heating elements were energized to heat particular fuel rods to a temperature differential of approximately 50 F above the temperature of the remainder of the bundle. This temperature differential was maintained for a specified time. At the completion of the test the furnace was cooled and the specimen removed. Bow values were again measured (on the same rods) and recorded at room temperature. The above procedure was repeated until measured increases in bow values as a function of time became very small. The total time of the specimen in the furnace at reactor temperatures approached 700 hours.

For the room temperature experiments, initial fuel rod bow values between ferrule planes were measured and recorded at bundle temperature for selected fuel rods. Hot water was circulated through selected fuel rods to obtain specified temperature differentials. Temperature differentials were set at 57 F, 74 F, and 120 F. At each temperature differential, rod bow values between ferrule planes were measured and

recorded. In addition to investigating fuel rod bowing characteristics at a steady temperature differential, the temperature differentials were cycled and bows recorded to determine the effect of repeated load application.

Also, at room temperature, the ferrule joints on specified fuel rods were cut at one ferrule plane to double unsupported column length of the rod. A temperature differential of 74 F was then applied to investigate the fuel rod bow due to loss of this transverse support. (74 F $\Delta T$ in the cold test is calculated to give the same deflection as 50 F $\Delta T$ in the reactor.) In the same test some rods were tested with only one attaching ferrule cut through.

The autoclave test consisted of placing fuel rod specimens (previously subjected to a braze cycle) of the same size and effective length (determined by vibratory frequency) as a fuel rod in the bundle into an autoclave producing temperature (650 F) and pressure (1800 psig). A mechanical axial load was applied to the specimen and, through the use of probes, the deflection (bow) of the specimen was determined.

Both the hot and cold test bundles were measured before and after testing to determine: the minimum clearance envelope, the warpage, the over-all bow, and the cross sectional dimensions.

## 4. RESULTS

### Reactor Temperature Bundle Test

Figure C-1 shows the data from the high temperature test and is the ratio of residual bow to manufactured bow for the hotter rods plotted against manufactured bow. The final (after 700 hours) residual bow readings are used. The curve drawn is an envelope curve and represents the maximum permanent fuel rod bow resulting from a sustained temperature differential applied at reactor operating temperature.

### Room Temperature Bundle Test

Figure C-2 represents the ratio of bow in the heated rods to the initial bow versus the initial bow. Bow was measured and recorded after one and 100 cycles of the applied temperature differential. The curve drawn is an envelope curve and represents the maximum fuel rod bow resulting from the applied temperature differential of 74 F.

Figure C-3 is a curve of manufactured fuel rod bow versus operating bow at the end of core life. The curve drawn is an envelope curve taken from Figures C-1 and C-2, and represents the fuel rod bow at reactor operating conditions for a range of manufactured fuel rod bow.

Figure C-4 is a plot of load versus deflection for individual fuel rod specimens subjected to axial column loads at 1800 psig and 650 F.

Broken Ferrule Test (Room Temperature Bundle)

Measurements of fuel rod bow in mils for a temperature differential of 74 F applied to the specimen at room temperatures and including loss of one ferrule support are 10.3, 12.2, 1.3 and 5.2. Identical measurements for loss of all ferrule support in one plane, which doubles the effective fuel rod column length, are. 14.2, 45.1, 38.3, 8.0 and 11.2.

Dimensional Changes

The maximum change in clearance envelope, before and after testing was 6 mils for either specimen.

## 5. DISCUSSION

All testing was based on a maximum temperature difference of 96 F between adjacent fuel rods. This difference occurs in the center spans of the corner rods and includes hot channel, flux peaking, and overpower factors. Since the center spans are filled with thorium oxide pellets, the corner rods are cooler; are in tension; and are not subject to column bowing. The adjacent rods are in compression. An averaging process which accounts for all the surrounding rods indicates the two (adjacent) rods are effectively 50 F hotter than their environment. The 50 F difference is used in the reactor temperature bundle tests.

It was desired to apply the bows from the room temperature bundle tests directly to the reactor. A calculation was performed to determine the temperature difference in a cold bundle which gives the same bow as 50 F $\Delta T$ gives in a hot test. The calculation accounts for the elastic nature of the cold rods as opposed to the plastic nature of the hot rods,

and indicates that a difference of 74 F should be used in the cold test.

Reactor Temperature Bundle Test

This test was terminated after 700 hours. At that time the time rate of bow increases was constant and very low. The temperature difference used was based on an overpower condition and it was not considered necessary to extrapolate the curve further. There is no anticipation of more than 700 hours at overpower during a single core life.

The thermal loading is probably conservative because of the lack of reactor pressure during this test. Reactor pressure produces an axial compressive stress in the fuel rods which is roughly equal to the proportional limit. Thermal compressive strains are absorbed in the plastic range of the material and produce lower stresses (and therefore loads) than they would in an elastic material.

Room Temperature Bundle Test

This test was run at temperature differences of 50 F and 115 F in addition to the 74 F discussed above. This helped obtain a plot of bow versus temperature difference. An effort to determine the temperature difference which would fail the braze joints was rather unsuccessful. The test apparatus limit of 115 F produced very little (if any) damage to the bundle. The same was true of 100 cycles run at 74 F difference.

Combining of Results of the Hot and Cold Bundle Tests

All of the required bundle test data would have been available from the high temperature test if it has been possible to take measurements at temperature; however, the complications of making measurements inside the furnace were too great. The high temperature test does show the effects of creep or relaxation over a period of time. If the manufactured bow in a rod is known, the results of the high temperature test show how much that rod would bow at the end of the core life in a cold condition. They do not show how much bow was in the rod during reactor operation. The room temperature test gives operating bow as a function of initial bow, and proper combination of the two tests permit determination of the operating bow at the end of the core life as follows:

1. If a rod has a manufactured bow of 0.006 inch, Figure 1 shows that at the end of core life the bow will have increased by a factor of about 2.65:1 to 0.016 inches with no load. If a 50 F thermal load were applied at that time, Figure 2 indicates that the bow would increase by about 1.5.1 to 0.024 inches.
2. If the operating bow at the beginning of core life were required, only Figure 2 need be consulted. An initial bow of 0.006 inch increases by a factor of about 2.2:1 to about 0.013 inches.

The results of a series of such calculations have been plotted as Figure 4. The shape of the curve of Figure 4 is probably misleading. It is reasonable to assume that operating bow is not independent of larger manufactured bows, and the curve probably increases in slope to a value of 1 at about 0.023 inch manufactured bow. For small manufactured bows the column effects are important. With increasing manufactured bow the column effects become less important (although sooner than expected) and probably have a final slope of 1 indicating an indifference to thermal loads.

At the time of the tests the allowable bow to prevent excessive blockage of the coolant flow channels was known to be greater than 0.027 inch and a 12% margin over this conservative test approach existed. Since that time, the unsupported span has been increased slightly by removing one ferrule plane, and the allowable bow increased by more refined calculations in proportion to the length ratio squared. The equivalent temperature difference between adjacent rods has been decreased from 50 F to 41 F, and makes the results even more conservative. A degree of conservatism is also introduced by combining the envelope curves from the hot and cold tests, each of which represents the worst data found in the individual tests.

To make it usable, the curve of Figure 2 has been extrapolated beyond the actual data points. This is the result of not having rods with large manufactured bows in the test bundle. The shape of the curve follows that found on the test work performed on another reactor for which points were available up to 0.013 inch of initial bow.

It should be noted that a stress strain curve is used to calculate the loads produced by the thermal differentials. A 50 F differential

produces a stress (load) which is over the proportional limit of the material at 650 F, and consequently the load increase is not proportional to the thermal differential increase. For instance, an increase from 50 F to 100 F (100%) produces only a 22% increase in load. Thus, the thermal margins of safety are greater than the load margins of safety in this load range.

Room Temperature Broken Ferrule Bundle Test

The broken ferrule tests indicated that a single broken joint had no effect on bow, but a complete loss of support at one ferrule plane caused a substantial increase in bow. The fuel element specification reflects this information and requires a minimum of 2 good braze joints for each rod in any ferrule plane.

Autoclave Test

This test was performed to determine reactor pressure effects on bow. The reactor design pressure of 1800 psig has no harmful effects on bow. The mechanical load equivalent for 50 F $\Delta T$ is 113 pounds and produces bow increases of 0.004 inch as shown on Figure 4. The initial bows could not be measured for this test and are unknown. However, the amount of bow increase is not sensitive to the initial bow (see Fig. 2) and initial bows of 0.001 inch to 0.015 inch attain increases under load of 0.005 inch to 0.007 inch. This excellent agreement between the cold bundle test and the hot autoclave test confirms the calculations of equivalent loads in both tests.

# APPENDIX D
# FUEL ROD VIBRATION TEST SUMMARY

## 1. OBJECTIVES

Fuel rods may vibrate as beams between ferrule support planes during reactor operation due to coolant flow excitation. This vibration may cause fuel rod or ferrule fatigue failure. A lack of sufficient confidence in analytical methods of predicting vibration amplitudes required resolution of the following items by test work.

1. The damped vibratory characteristics of a fuel rod filled with fuel pellets of unknown dynamic qualities.
2. The effects of fuel rod end restraint.
3. The fatigue life characteristics of a brazed ferrule-fuel rod assembly of uncertain mechanical properties.

## 2. CONCLUSIONS

The maximum predicted vibratory amplitudes are well below the amplitudes required to produce fatigue failure in the clad. The predicted vibratory amplitude is less than 1 mil while a comparable amplitude for $10^7$ cycles fatigue life is 4.9 mils.

The magnification ratio of a fuel rod is about 1.4 to 2 if the fuel load has the consistency of coarse dry sand or lead filings.* A magnification ratio of 5 or less is considered satisfactory; hence the fuel rods will be indifferent even to resonant excitation.

## 3. DESCRIPTION

Two types of bench tests were performed: (1) a rotating beam type fatigue test was performed on fabricated bundle subsections; (2) an instantaneous excitation vibration test was performed on subsections cut from a prototype bundle.

*Magnification ratio is the ratio of dynamic amplitude to static amplitude (deflection) of a member, for identical loading.

Fatigue Test

Specimens were designed to simulate a section of an individual fuel pin with its attachment and support in the fuel bundle. The main pin to be flexed (rotated) was 10-1/4 inches long and was surrounded at one end by four ferrules which in turn were surrounded by eight 2 inch fuel pin sections. The specimen was mounted rigidly by bolts through the four corner (2 inches long) fuel pin sections. The centerline of the opposite end of the 10-1/4 inch long rod was then rotated in a circle with a radius equal to the test amplitude. The test determined the amplitude to produce a failure at $10^6$ and $10^7$ cycles. Strain gages in two planes on the 10-1/4 inch rod provided data for the calculation of the stress at the plane of failure.

Vibration Test

The specimen for this test was cut from a prototype bundle. It consisted of four fuel rods, each with a length of three ferrule planes, and twelve fuel rods, 1 3/4 inches in length, attached at each ferrule plane by ferrules. A long fuel rod was struck with a rubber hammer. The resulting sound was picked up by microphone, then displayed and photographed on an oscilloscope. Several series of these tests were made with fuel rod loadings of lead filings, sand, and mercury. The result was a plot of amplitude of vibration versus number of cycles for each loading from which magnification ratio for differing fuel rod loadings could be calculated.

## 4. RESULTS

The results of the reverse bend tests are shown in Figure D-1 which is plotted as amplitude and stress versus cycles to failure. The data points shown with arrows indicate the specimens had not failed at the given number of cycles. They were removed because they had satisfied the test aims. The failures all occurred in the long fuel rod immediately adjacent to the ferrule cluster attachment. Figure D-1 indicates that a $10^7$ cycles fatigue life can be expected for 110 mils amplitude 10-1/4 inches from the ferrule cluster attachment.

The photographic results from the vibration test indicate that the magnification ratio of a fuel rod is in the order of 1.4 to 2.0 for a fuel

load with the consistency of coarse dry sand or lead filings. A tabular summary of these results is shown in Table D-1.

The vibratory midspan amplitude of an individual fuel rod influenced by a parallel flow of water was calculated from the following expression*.

$$(y/d)^{1.3} = 0.83 \times 10^{-10} K \left(\frac{\rho_w V^2 L^4}{EI}\right)^{1/2} \frac{(\rho_w V^2)}{\mu^{\omega}}$$

Where

$y$ = Rod midspan deflection
$d$ = Hydraulic diameter
$K$ = Factor for end fixity
$\rho_w$ = Density of water
$V$ = Water flow velocity
$L$ = Rod length
$E$ = Modulus of elasticity
$I$ = Rod moment of inertia
$\mu$ = Viscosity of water
$\omega$ = Frequency of rod vibration

The maximum calculated amplitude is 0.6 mils using operating temperature values and reference design physical values.

## 5. DISCUSSION

The preceding calculation indicated the maximum vibratory amplitude of the fuel rod midspan will not exceed 0.6 mils. The following compares this calculated deflection with the results of the reverse bending tests.

It is assumed that a fuel rod between ferrules is a beam, "fixed" at both ends, and that the vibratory deflected shape is the same as the deflected shape of a beam with uniformly distributed loading. These assumptions are conservative because the stresses are highest for a "fixed" end beam with distributed loading for any given deflection. The following standard formulas apply to such a beam:

*D. Burgreen, J. J. Byrnes and D. M. Benforado "Vibration of Rods Influenced by Water in Parallel Flow" Trans. ASME 80 7-1958 No. 5, Page 991.

$$\delta = \frac{W L^3}{384EI} \quad (1)$$

$$M = \frac{W L}{12} \quad (2)$$

$$S = \frac{MC}{I} \quad (3)$$

Combining these expressions produces the following expression for deflection in terms of stress.

$$\delta = \frac{SL^2}{32EC} \quad (4)$$

Figure D-1 indicates a stress of 12,000 psi for the $10^7$ cycles fatigue life. This testing was performed at room temperature. Similar work on another contract indicated that the fatigue life stress at 650 F is not less than 82% of the room temperature value, or 9,850 psi in this case. This fatigue life stress plus reference design mechanical values are substituted in Equation (4). The solution yields $\delta = 4.9$ mils which is the indicated vibratory amplitude to produce a stress equal to the $10^7$ cycles fatigue life stress.

The calculation of a vibratory amplitude of 0.6 mils does not include any factors for the damping effect of the fuel pellets. Although the results of the fatigue life test indicate a considerable margin of safety ($4.9/0.6 = 8$), this damping effect was investigated.

The form the fuel pellets will take during operation is unknown. They may be uncracked or cracked into unknown size pieces. The testing was performed on materials which span any anticipated operating condition of the fuel pellets in the reactor. Three fuel rod loading materials were selected, lead filings, coarse sand, and mercury, and it was expected that the damping effects would be descending in the order listed. This is borne out by the results in Table D-I. The fuel is expected to behave more like the sand and filings than the mercury, and the actual magnification factor (ratio of dynamic to static deflections under the same load) should be less than 2. This indicates the fuel rods will not respond appreciably even to resonant excitation.

TABLE D-I

| Specimen | Load Material | Magnification Factor |
|---|---|---|
| 1 | Lead Filings | 1.43 |
| 2 | Coarse Sand | 1.72 |
| 3 | Mercury | 5.75 |

# APPENDIX E
# PRESSURE AND TEMPERATURE CYCLE TEST SUMMARY

## 1. OBJECTIVES

The test is a demonstration of the ability of the lip welded hemispherical plug end closure design to withstand maximum anticipated transient operating conditions.

## 2. CONCLUSIONS

The fuel rod cladding end closure will withstand the maximum anticipated heating and cooling rates during reactor operation. Test conditions were more severe than the maximum anticipated reactor operating conditions.

## 3. DESCRIPTION

Fuel rod tubes provided with welded end caps and subjected to a simulated braze cycle were leak checked to determine end closure weld integrity. The test specimen was then subjected to fast temperature and pressure cycles and leak checked again.

## 4. RESULTS

No failures or indications of leakage were observed after testing. The results are conservative since the test utilized an end cap design with more thermal inertia than the reference design. Figure E-I shows the temperature and pressure cycles used during testing. Table E-I summarizes the results of the temperature and pressure cycling test.

TABLE E-I

SUMMARY OF FUEL ROD END CLOSURE PRESSURE AND TEMPERATURE CYCLING TEST

| Number of Cycles | Leakage | Type of Leak Test | Maximum Heating Rate, F/min | Maximum Cooling Rate, F/min |
|---|---|---|---|---|
| 175 | None | Mass spectrograph before and after | 300 | 1200 |
| 180 | None | Liquid soap before and after | 300 | 1200 |
| 210 | None | Liquid soap before and after | 300 | 1200 |
| 286 | None | Liquid soap before Mass spectrograph after | 300 | 1200 |
| 433 | None | Liquid soap before Mass spectrograph after | 300 | 1200 |
| 1160 | None | Liquid soap before Mass spectrograph after | 300 | 1200 |

# APPENDIX F

## KANIGEN AND NICROBRAZE 50 STRENGTH TEST SUMMARY

### 1. OBJECTIVES

A comparison of the strength of brazed joints fabricated with Kanigen and Nicrobraz 50 materials is required.* (The composition of Kanigen and Nicrobraz 50 is given in Table F-I.)

### 2. CONCLUSIONS

Test results indicate no significant difference in strength between Kanigan and Nicrobraz 50 joints.

Test of brazed joint integrity show the ferrule to clad joints of either the Kanigen brazed or the Nicrobraz 50 brazed fuel bundle will withstand the worst anticipated loads produced by thermal differentials between fuel rods. The number of joint failures which might statistically be expected is insignificant in relation to the over-all fuel element structural integrity.

Fuel rod attachment fatigue tests show the brazed ferrule to clad joint (with either Kanigen or Nicrobraz 50) is stronger than the cladding itself when subjected to cycle loading. The Kanigen brazed joint is slightly more fatigue resistant than the Nicrobraze 50 brazed assembly.

### 3. RESULTS

The results of the cold $\Delta T$ test are given in Table F-II. The results of the hot $\Delta T$ test are given in Table F-III. The results of reverse bending fatigue tests on 14 specimens brazed with Nicrobraz 50 and 12 specimens brazed with Kanigen are compared in Table IV.

*Kanigen — Trade name of General American Transportation Company.
Nicrobraz — Trade name of Wall-Colmonoy Corporation.

TABLE F-I

COMPOSITION OF KANIGEN AND NICROBRAZE 50

| Material | Composition, % Nickel | Phosphorus | Chrome |
|---|---|---|---|
| Kanigen | 90 | 10 | — |
| Nicrobraze 50 | 77 | 10 | 13 |

TABLE F-11

COMPARISON OF KANIGEN AND NICROBRAZ 50 JOINTS COLD ΔT TEST

| Braze Material | Number of Unbrazed Joints Prior to Testing | Number of Broken Joints After Testing | Total Unattached Joints After Testing |
|---|---|---|---|
| Kanigen | 3 of 968 = 0.31%[1] | 29 of 1431 = 2%[2] | 39 of 1431 = 2.7%[2] |
| Nicrobraz 50 | 104 of 1190 = 8.7%[3] | 42 of 1190 = 3.5%[2] | 146 of 1190 = 12.2%[2] |

[1] Indicates inspection by Borescope.

[2] Indicates visual inspection after sectioning.

[3] These joints had no braze material when inspected after sectioning. It is assumed this was also the situation before testing.

TABLE F-III

COMPARISON OF KANIGEN AND NICROBRAZ 50 JOINTS

HOT ΔT TEST

| Braze Material | Number of Unbrazed Joints Prior to Testing | Number of Broken Joints After Testing |
|---|---|---|
| Kanigen | 18 of 468 = 3.8%[1] | None[1] |
| Nicrobraz 50 | 5 of 834 = 0.6%[1] | 1 of 834 = 0.12%[2] |

[1] Indicates inspection by Borescope.

[2] Indicates visual inspection after sectioning.

TABLE IV

COMPARISON OF REVERSED BENDING TESTS

| Material | Reverse Bending Amplitude, mils | |
|---|---|---|
| | Failure at $10^6$ Cycles | Failure at $10^7$ Cycles |
| Nicrobraz 50 | 75 | 50 |
| Kanigen | 75 | 65 |

Note: All failures were in the rod at the start of the braze fillet.

FIG. C-1: HIGH TEMPERATURE BUNDLE TEST

(Residual Bow/Manufactured Bow Vs Manufactured Bow)

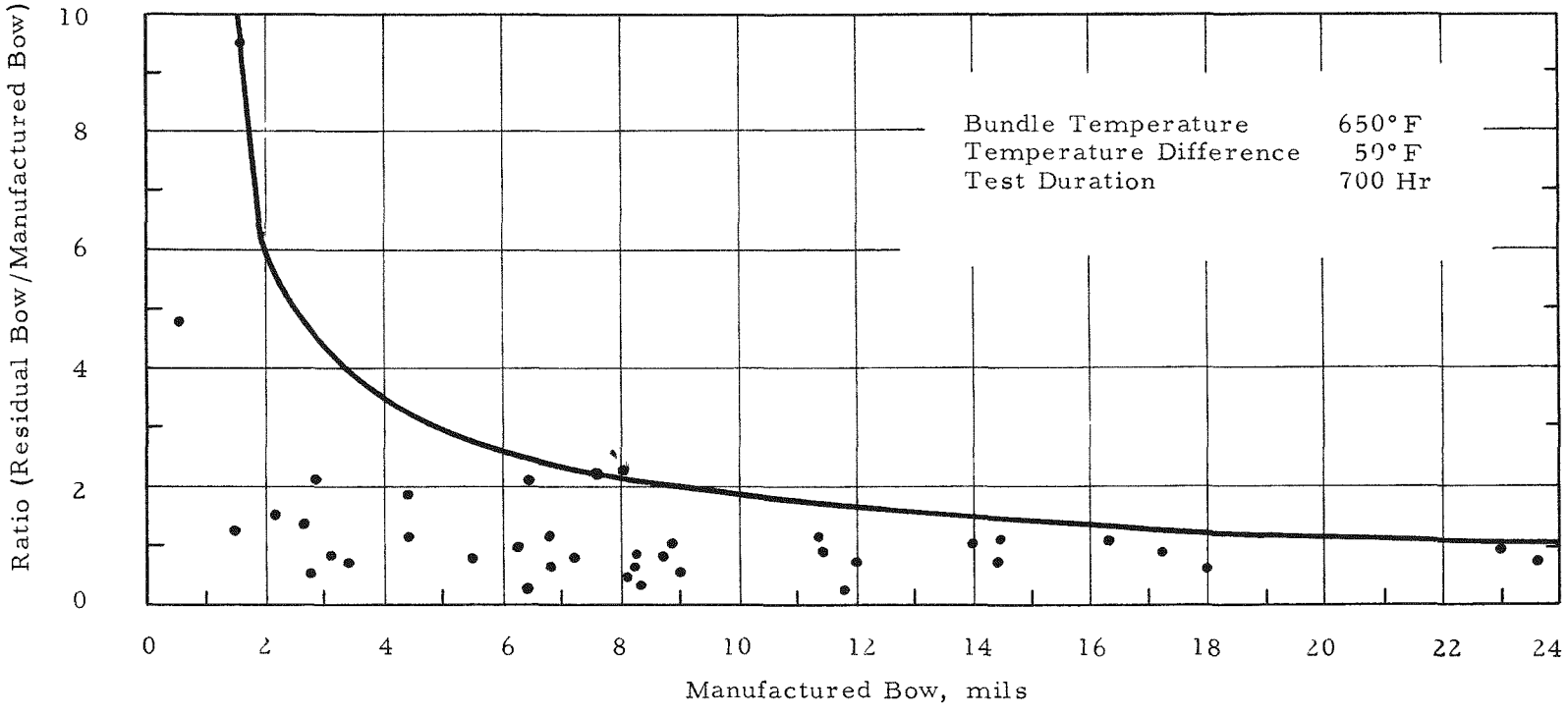

FIG. C-2: ROOM TEMPERATURE BUNDLE TEST

(Final Bow/Initial Bow Vs Initial Bow)

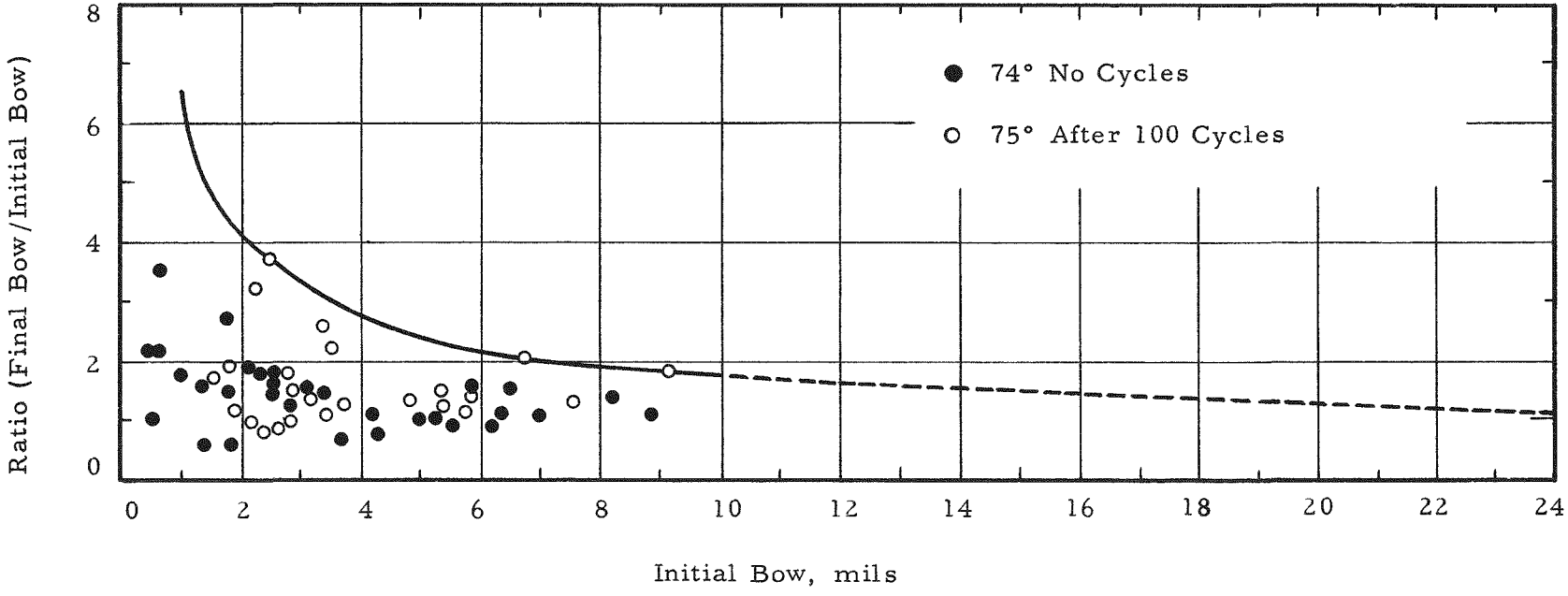

FIG. C-3: OPERATING VS MANUFACTURED BOW

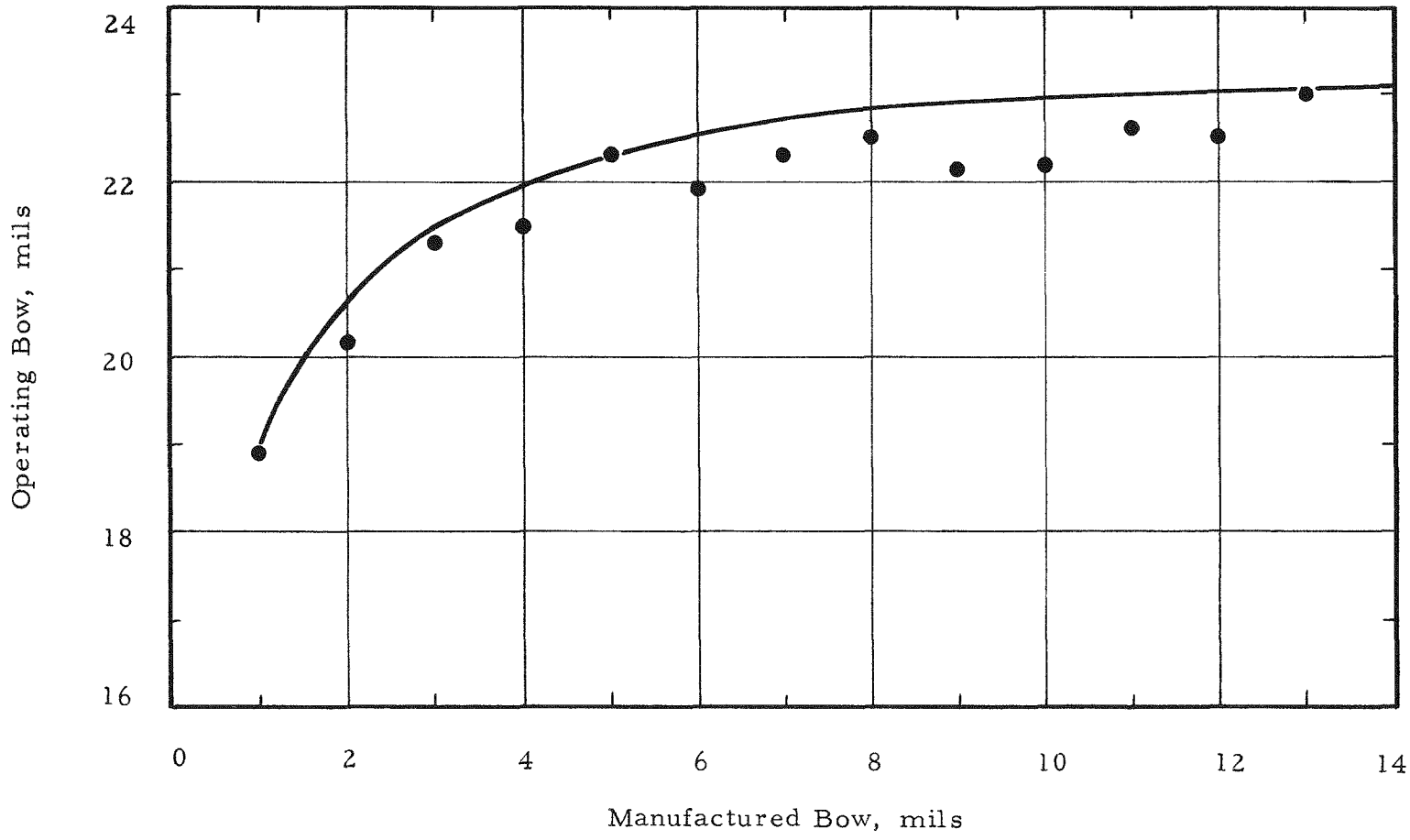

FIG. C-4: AUTOCLAVE TEST OF INDIVIDUAL RODS

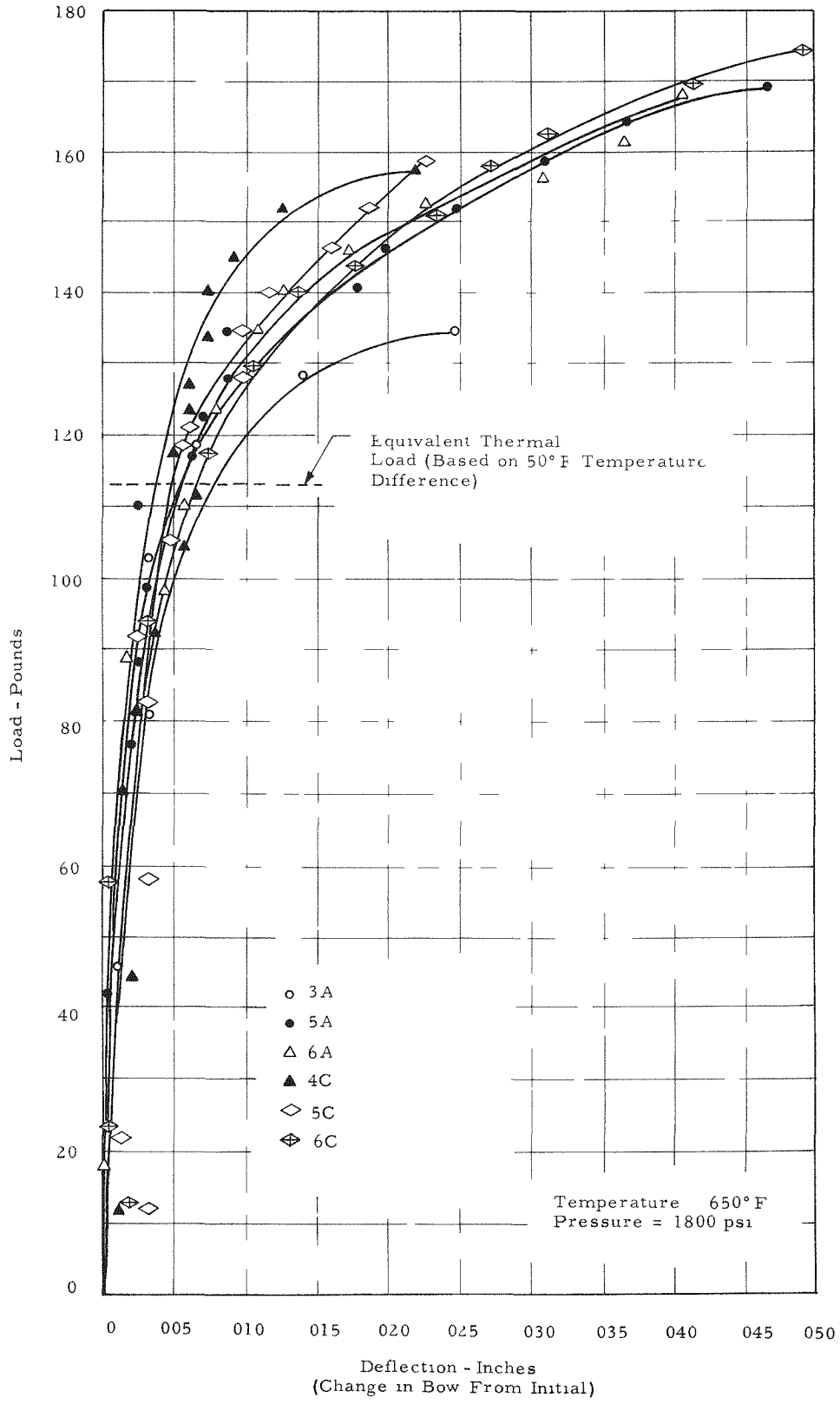

FIG. D-1: STRESS AND STRAIN VS NUMBER OF CYCLES TO FAILURE

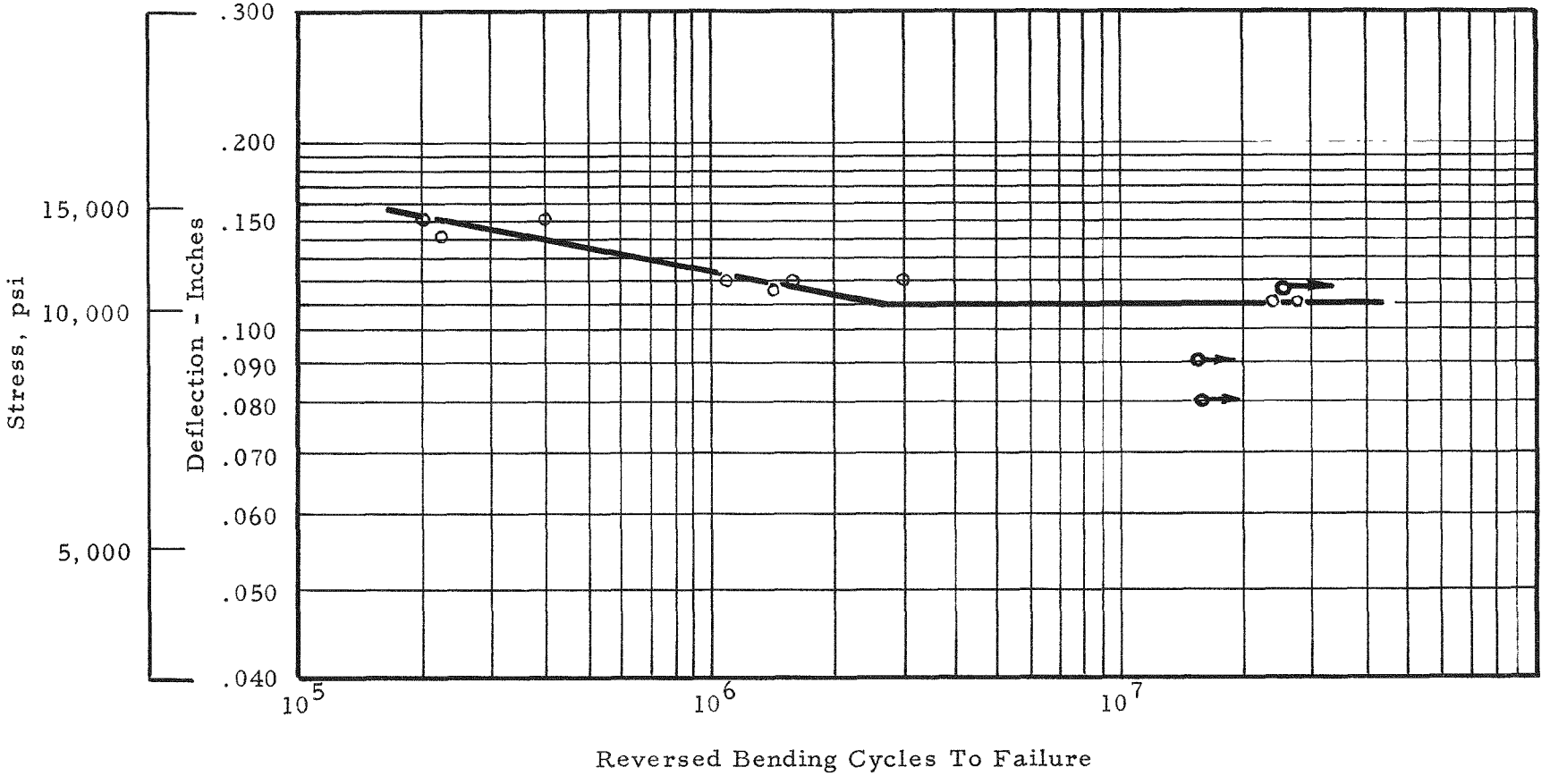

FIG. E-1: PRESSURE AND TEMPERATURE CURVES

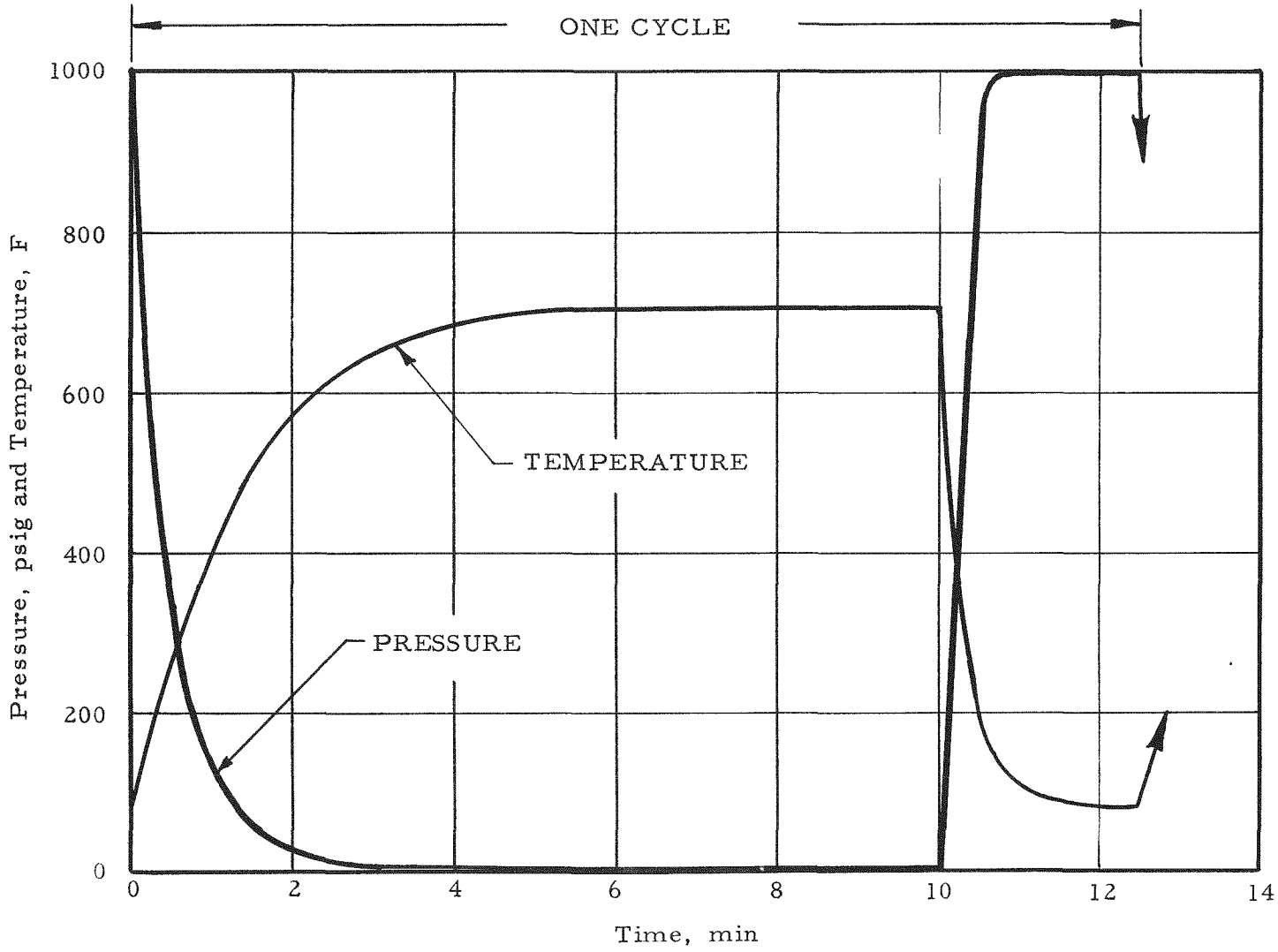


537-077